

June 1999

hep-ph/9906215
MSUHEP-90523

New Physics in the Third Family and its Effect on Low Energy Data

Ehab Malkawi^{a,1} and C.-P. Yuan^b^aDepartment of Physics, Jordan University of Science & Technology
Irbid 22110, Jordan^bDepartment of Physics and Astronomy, Michigan State University
East Lansing, MI 48824, USA**Abstract**

We investigate, in detail, a model in which the third family fermions are subjected to an SU(2) dynamics different from the first two families. Constrained by the precision Z -pole data, the heavy gauge boson mass is bounded from below to be about 1.7 TeV at the 2σ level. The flavor-changing neutral current (FCNC) in the lepton sector can be significant in $\tau \leftrightarrow e$ and $\tau \leftrightarrow \mu$ transitions. In the latter case, the ratio $\text{Br}(\tau \rightarrow \mu \bar{\nu}_\mu \nu_\tau) / \text{Br}(\tau \rightarrow e \bar{\nu}_e \nu_\tau)$ and $\text{Br}(\tau \rightarrow \mu \mu \mu)$ can constrain the model better than LEP/SLC data in some region of the parameter space. Furthermore, FCNCs are unavoidable in the quark sector. Significant effects to the $B^0\text{--}\bar{B}^0$ mixing and the rare decays of the K and B mesons, such as $K^\pm \rightarrow \pi^\pm \nu \bar{\nu}$, $b \rightarrow s \nu \bar{\nu}$, $B_s \rightarrow \tau^+ \tau^-$, $\mu^+ \mu^-$ and $B_{s,d} \rightarrow \mu^\pm \tau^\mp$, are expected.

PACS numbers:12.15.Ji, 12.60.-i, 12.60.Cn, 13.20.-v, 13.35.-r

¹e-mail:malkawie@just.edu.jo

1 Introduction

The search for physics beyond the Standard Model (SM) is an ongoing endeavor. Usually, a search for new physics implies investigating higher and higher energy regime where new physics effects are expected to appear. Nevertheless, it remains a necessary and useful approach to study the low-energy regime where interesting phenomena may be expected in a particular model. The work presented here is an example where new physics diminishes in some of the very low-energy processes and flourishes in the others.

The flavor physics of the third generation is particularly mysterious for the smallness of the mixing angles and the huge hierarchy in masses. Furthermore, the heavy top quark mass can be an indication for a new dynamics in the third fermion generation different from the first two generations. It is interesting to investigate the idea of treating the third generation differently from the first two generations in the context of strong or electroweak interactions. Fortunately, the already available low energy data can largely constrain such a picture. In this regard, several studies have been pursued in the literature. In the context of the Quantum Chromodynamics (QCD) interaction, we refer the reader to Refs. [1, 2]. In the context of the electroweak interaction, several published works also exist. As an example, in the context of Technicolor theories, we refer the reader to Ref. [3]. The idea that the third generation carries a separate $SU(2)$ was proposed in Refs. [4, 5, 6]. The two models in Refs. [5, 6] differ in the assignment of the quantum numbers to the Higgs sector which leads to different phenomenological implications. Constraints from low energy data on such models have been discussed in Refs. [5, 6, 7, 8].

In Ref. [5], we proposed a model in which the third generation feels a different gauge dynamics (with a new $SU(2)$ gauged symmetry) from the usual weak interaction proposed in the SM. (No modification to the QCD interaction was considered, because that case has been discussed elsewhere [1, 2].) Consequently, a new spectrum of gauge bosons emerges in the model. We, then, used the available CERN Large Electron Positron (LEP) and SLAC Stanford Linear Collider (SLC) data to constrain the parameters of the model. We found the model to be consistent with data (at the 3σ level) as long as the heavy gauge boson mass is larger than 1.3 TeV. A similar conclusion was also found in Refs. [6, 7, 8].²

In this current work, we first update the previous analysis on constraining the parameter space of the proposed model using the most recent LEP and SLC data [9], then discuss the zero-momentum transfer physics in the low-energy regime where interesting effects may be expected in both lepton and quark sectors. We find that flavor-changing neutral currents (FCNCs) may exist in the lepton sector and are unavoidable in the quark sector. As a consequence, neutrinos can mix via gauge interaction despite of their zero mass. Furthermore, deviations from the SM predictions are expected for some particular low-energy processes. For example, the decay process $\tau \rightarrow \mu \bar{\nu}_\mu \nu_\tau$ can impose a stronger constraint than the Z -pole data for some particular parameter space. Similarly, the B^0 - \bar{B}^0 mixing and the rare decay rates

² Though, the assignment of the fermion quantum numbers may not be identical.

of the K and B mesons, such as $K^\pm \rightarrow \pi^\pm \nu \bar{\nu}$ and $B_s \rightarrow \tau^+ \tau^-, \mu^+ \mu^-$ are expected to exceed the SM prediction for some region of the parameter space. Non-SM decay modes, such as $B_{s,d} \rightarrow \mu^\mp \tau^\pm$, can also occur.

The rest of this paper is organized as follows. In Sec. 2, we briefly review the model. In Sec. 3, we discuss the constraints on the model from the Z -pole data at LEP and SLC. After a general discussion on the possible new effects on low energy data in Sec. 4, we discuss all possible new physics effects, including all FCNC processes as predicted by this model, in Secs. 5 and 6. We summarize our conclusions in Sec. 7.

2 The Model

For the detailed structure of the model, we refer the reader to Ref. [5]. In this section we only outline the main features of the proposed model. The model is based on the gauge symmetry $G = SU(2)_l \times SU(2)_h \times U(1)_Y$. The third generation of fermions (top quark, t , bottom quark, b , tau lepton, τ , and its neutrino, ν_τ) experiences a new gauge interaction, instead of the usual weak interaction advocated by the SM. On the contrary, the first and second generations only feel the weak interaction supposedly equivalent to the SM case. The new gauge dynamics is attributed to the $SU(2)_h$ symmetry under which the left-handed fermions of the third generation transform in the fundamental representation (doublets), while they remain to be singlets under the $SU(2)_l$ symmetry. On the other hand, the left-handed fermions of the first and second generation transform as doublets under the $SU(2)_l$ group and singlets under the $SU(2)_h$ group. The $U(1)_Y$ group is the SM hypercharge group. The right-handed fermions only transform under the $U(1)_Y$ group as assigned by the SM. Finally the QCD interactions and the color symmetry $SU(3)_C$ are the same as that in the SM.

The symmetry breaking of the Lie group G into the electromagnetic group $U(1)_{\text{em}}$ is a two-stage mechanism. First, $SU(2)_l \times SU(2)_h \times U(1)_Y$ breaks down into $SU(2)_L \times U(1)_Y$ at some large energy scale. The second stage is that $SU(2)_L \times U(1)_Y$ breaks down into $U(1)_{\text{em}}$ at an energy scale about the same as the SM electroweak symmetry-breaking scale. The spontaneous symmetry-breaking of the group $SU(2)_l \times SU(2)_h \times U(1)_Y$ is accomplished by introducing two scalar matrix fields Σ and Φ which transform as

$$\Sigma \sim (2, 2)_0, \quad \Phi \sim (2, 1)_1,$$

i.e., the Σ field transforms as a doublet under both $SU(2)_l$ and $SU(2)_h$ and as a singlet under $U(1)_Y$. On the other hand, the Φ field transforms as a doublet under $SU(2)_l$, as a singlet under $SU(2)_h$, and its hypercharge quantum number Y is 1. Thus, the scalar doublet Φ carries equivalent quantum numbers as the SM Higgs doublet.

As a realization of the symmetry, the Σ and Φ fields transform as

$$\Sigma \rightarrow g_1 \Sigma g_2^\dagger, \quad \Phi \rightarrow g_1 g_Y \Phi,$$

where $g_1 \in SU(2)_l$, $g_2 \in SU(2)_h$, and $g_Y \in U(1)_Y$. For completeness, we briefly discuss the structure of the boson and lepton sectors as follows.

2.1 The Boson Sector

The covariant derivatives of the scalar fields are defined as

$$\begin{aligned} D^\mu \Sigma &= \partial^\mu \Sigma + ig_l W_l^\mu \Sigma - ig_h \Sigma W_h^\mu, \\ D^\mu \Phi &= \partial^\mu \Phi + ig_l W_l^\mu \Phi + \frac{i}{2} g' B^\mu \Phi, \end{aligned} \quad (1)$$

where $W_{l,h} \equiv W_{l,h}^a \tau^a / 2$ and where $W_{l,h}^a$ are the gauge boson fields of the $SU(2)_{l,h}$ groups, respectively. (τ^a 's are the Pauli matrices, and $\text{Tr}(\tau^a \tau^b) = 2\delta_{ab}$.)

With these definitions, the gauge invariant Lagrangian of the boson sector is

$$\begin{aligned} \mathcal{L}_B &= \frac{1}{2} D_\mu \Phi^\dagger D^\mu \Phi + \frac{1}{4} \text{Tr}(D_\mu \Sigma^\dagger D^\mu \Sigma) + V(\Phi, \Sigma) \\ &\quad - \frac{1}{4} W_{l\mu}^a W_l^{a\mu} - \frac{1}{4} W_{h\mu}^a W_h^{a\mu} - \frac{1}{4} B_\mu B^\mu, \end{aligned} \quad (2)$$

where $V(\Phi, \Sigma)$ is the scalar potential. We assume that the first stage of symmetry breaking is accomplished through the Σ field by acquiring a vacuum expectation value (VEV) u , i.e., $\langle \Sigma \rangle = \begin{pmatrix} u & 0 \\ 0 & u \end{pmatrix}$. The second stage is through the scalar Φ field by acquiring a vacuum expectation value v , so $\langle \Phi \rangle = \begin{pmatrix} 0 \\ v \end{pmatrix}$, where v is at the same order as the SM symmetry-breaking scale. Because of this pattern of symmetry breaking, the gauge couplings are related to the $U(1)_{\text{em}}$ gauge coupling e by the relation

$$\frac{1}{e^2} = \frac{1}{g_l^2} + \frac{1}{g_h^2} + \frac{1}{g'^2}. \quad (3)$$

We then define

$$g_l = \frac{e}{\sin \theta \cos \phi}, \quad g_h = \frac{e}{\sin \theta \sin \phi}, \quad g' = \frac{e}{\cos \theta}, \quad (4)$$

where θ plays the role of the usual weak mixing angle and ϕ is a new parameter of the model. The scalar fields, except $\text{Re}(\phi^0)$ from the Φ doublet and σ from the $\Sigma (\equiv \sigma + i\pi^a \tau^a)$ matrix field, become the longitudinal components of the physical gauge bosons. The surviving $\text{Re}(\phi^0)$ field behaves similar to the SM Higgs boson except that it does not have the usual Yukawa couplings to the third generation.

To derive the mass eigenstates and physical masses of the gauge bosons, we need to diagonalize their mass matrices. For $g_h > g_l$ (equivalently $\tan \phi < 1$), we require $g_h^2 \leq 4\pi$ (which implies $\sin^2 \phi \geq g^2/(4\pi) \sim 1/30$) so that the perturbation theory is valid. Similarly, for $g_h < g_l$, we require $\sin^2 \phi \leq 0.96$. For simplicity, we focus on the region where $x (\equiv u^2/v^2)$ is much larger than 1, and ignore the corrections which are suppressed by higher powers of $1/x$. To the order $1/x$, the light gauge boson masses are found to be [5]

$$M_{W^\pm}^2 = M_0^2 \left(1 - \frac{\sin^4 \phi}{x} \right), \quad (5)$$

$$M_Z^2 = \frac{M_0^2}{\cos^2 \theta} \left(1 - \frac{\sin^4 \phi}{x}\right), \quad (6)$$

where $M_0 \equiv ev/2 \sin \theta$. While for the heavy gauge bosons, one finds

$$M_{W'^{\pm}}^2 = M_{Z'}^2 = M_0^2 \left(\frac{x}{\sin^2 \phi \cos^2 \phi} + \frac{\sin^2 \phi}{\cos^2 \phi} \right). \quad (7)$$

It is interesting to notice that up to this order the heavy gauge bosons are degenerate in mass. This is because the heavy gauge bosons do not mix with the hypercharge gauge boson field, B_μ .

2.2 The Fermion Sector

As discussed before, the third generation interacts with the $SU(2)_h$ gauge bosons, and the first and second generations interact with the $SU(2)_l$ gauge bosons. Explicitly, under the $SU(2)_l \times SU(2)_h \times U(1)_Y$ symmetry, the quantum numbers of the fermions are assigned as follows. For the first and second generation fermions, we assign

left-handed quarks : $(2, 1)_{1/3}$, left-handed leptons : $(2, 1)_{-1}$.

For the third generation, we have

left-handed quarks : $(1, 2)_{1/3}$, left-handed leptons : $(1, 2)_{-1}$.

For all the right-handed fermions, we assign

right-handed quarks and leptons : $(1, 1)_{2Q}$,

where Q is the electric charge of the fermions. Because of this assignment, the model is anomaly free, and the cancellation of anomalies is satisfied family by family.

In terms of the mass eigenstates of the gauge bosons W^\pm , Z , W'^\pm , and Z' , the fermionic interaction Lagrangian is

$$\begin{aligned} \mathcal{L}_f^{int} = & \frac{e}{\sin \theta} \overline{\Psi}_L \gamma^\mu \left[T_l^\pm + T_h^\pm + \frac{\sin^2 \phi}{x} (T_h^\pm \cos^2 \phi - T_l^\pm \sin^2 \phi) \right] \Psi_L W_\mu^\pm + \\ & \frac{e}{\sin \theta \cos \theta} \overline{\Psi}_L \gamma^\mu \left[T_l^3 + T_h^3 - Q \sin^2 \theta + \frac{\sin^2 \phi}{x} (\cos^2 \phi T_h^\pm - \sin^2 \phi T_l^\pm) \right] \Psi_L Z_\mu \\ & + \frac{e}{\sin \theta} \overline{\Psi}_L \gamma^\mu \left[-\frac{\sin \phi}{\cos \phi} T_l^\pm + \frac{\cos \phi}{\sin \phi} T_h^\pm - \frac{\sin^3 \phi \cos \phi}{x \cos^2 \theta} (T_h^\pm + T_l^\pm) \right] \Psi_L W_\mu'^\pm + \\ & \frac{e}{\sin \theta} \overline{\Psi}_L \gamma^\mu \left[-\frac{\sin \phi}{\cos \phi} T_l^3 + \frac{\cos \phi}{\sin \phi} T_h^3 - \frac{\sin^3 \phi \cos \phi}{x \cos^2 \theta} (T_h^3 + T_l^3 - Q \sin^2 \theta) \right] \Psi_L Z'_\mu \\ & + eQ \bar{f}^i \gamma^\mu f^i A_\mu - \frac{eQ \sin^2 \theta}{\sin \theta \cos \theta} \bar{f}_R^i \gamma^\mu f_R^i \left(Z_\mu - \frac{\sin^3 \phi \cos \phi}{x \cos \theta} Z'_\mu \right). \end{aligned} \quad (8)$$

The first and second generations acquire their masses through the Yukawa interactions to the Φ doublet field. The fermions Yukawa Lagrangian is

$$\begin{aligned} \mathcal{L}_{\text{Yukawa}} = & \overline{\Psi}_L^1 \Phi [g_{11}^e e_R + g_{12}^e \mu_R + g_{13}^e \tau_R] + \\ & \overline{\Psi}_L^2 \Phi [g_{21}^e e_R + g_{22}^e \mu_R + g_{23}^e \tau_R] + h.c. \end{aligned} \quad (9)$$

For the third generation one cannot generate their masses through the usual Yukawa terms (dimension-four operators), as it is not allowed by gauge invariance. This can be an indication that the mass generation of the third family is due to a different mechanism than the first two generations. One way to realize this is to assume that our proposed symmetry can be embedded in a larger symmetry at a much higher energy scale. The breaking of the large symmetry is responsible for the generation of the third family masses as it is also responsible for the new non-universal gauge dynamics. At the low energy scale this can be effectively written in terms of higher dimension operators. For example, the mass of the τ lepton can be generated through the following dimension-five operators:

$$\frac{1}{\Lambda} \overline{\Psi}_L^3 \Sigma^\dagger \Phi [g_{31} e_R + g_{32} \mu_R + g_{33} \tau_R] + h.c., \quad (10)$$

where $\Psi_L^3 = \begin{pmatrix} \nu_{\tau L} \\ \tau_L \end{pmatrix}$, and Λ characterizes some large mass scale associated with the strong flavor interaction. It is reasonable to assume $\Lambda \sim u \gg v$, so that the mass of τ is about equal to $g_{33} v$. Thus, although the masses of the first and second generations are generated through the Yukawa interactions as in the SM, the mass spectrum of third generation must be generated by a different mechanism. This conclusion may be attributed to strong flavor dynamics which could be evident at high energies, where the interactions become strong. Another scenario [4] for generating the third family masses in this model is to introduce an additional scalar doublet which only couples to the third generation through the usual Yukawa interactions. In general, this scenario will introduce extra interaction terms to the gauge dynamics and will modify the conclusions presented in this paper.

Given the fermion mass matrices, one can derive their physical masses by diagonalizing the mass matrices using bilinear unitary transformations. For example, for the lepton sector, the lepton mass matrix M_e can be read out from the Lagrangian written above in Eqs. (9) and (10). We introduce the unitary matrices L_e and R_e with the transformations:

$$e_L^i \rightarrow L_e^{ij} e_L^j, \quad e_R^i \rightarrow R_e^{ij} e_R^j. \quad (11)$$

Hence, the physical mass matrix is given by

$$M_e^{\text{diag.}} = L_e^\dagger M_e R_e. \quad (12)$$

Because the third family interacts differently from the first and second generation, we expect in general flavor-changing neutral currents to occur at tree level.

In terms of the fermion mass eigenstates, the left-handed neutral-current interactions are

$$\frac{e}{2 \sin \theta \cos \theta} \begin{pmatrix} \overline{e}_L & \overline{\mu}_L & \overline{\tau}_L \end{pmatrix} \gamma^\mu \left[-1 + 2 \sin^2 \theta + \frac{\sin^4 \phi}{x} - \frac{\sin^2 \phi}{x} L_e^\dagger G L_e \right] \begin{pmatrix} e_L \\ \mu_L \\ \tau_L \end{pmatrix} Z_\mu,$$

$$\frac{e}{2 \sin \theta \cos \theta} \begin{pmatrix} \overline{\nu_{eL}} & \overline{\nu_{\mu L}} & \overline{\nu_{\tau L}} \end{pmatrix} \gamma^\mu \left[1 - \frac{\sin^4 \phi}{x} + \frac{\sin^2 \phi}{x} L_e^\dagger G L_e \right] \begin{pmatrix} \nu_{eL} \\ \nu_{\mu L} \\ \nu_{\tau L} \end{pmatrix} Z_\mu,$$

$$\frac{e}{2 \sin \theta} \begin{pmatrix} \overline{e_L} & \overline{\mu_L} & \overline{\tau_L} \end{pmatrix} \gamma^\mu \left[\frac{\sin \phi}{\cos \phi} + \frac{\sin^3 \phi \cos \phi}{x \cos^2 \theta} (1 - 2 \sin^2 \theta) - \frac{L_e^\dagger G L_e}{\sin \phi \cos \phi} \right] \begin{pmatrix} e_L \\ \mu_L \\ \tau_L \end{pmatrix} Z'_\mu,$$

$$\frac{e}{2 \sin \theta} \begin{pmatrix} \overline{\nu_{eL}} & \overline{\nu_{\mu L}} & \overline{\nu_{\tau L}} \end{pmatrix} \gamma^\mu \left[-\frac{\sin \phi}{\cos \phi} - \frac{\sin^3 \phi \cos \phi}{x \cos^2 \theta} + \frac{L_e^\dagger G L_e}{\sin \phi \cos \phi} \right] \begin{pmatrix} \nu_{eL} \\ \nu_{\mu L} \\ \nu_{\tau L} \end{pmatrix} Z'_\mu, \quad (13)$$

where

$$G = \begin{pmatrix} 0 & 0 & 0 \\ 0 & 0 & 0 \\ 0 & 0 & 1 \end{pmatrix}. \quad (14)$$

The left-handed charged-current interactions are

$$\frac{e}{\sqrt{2} \sin \theta} \begin{pmatrix} \overline{e_L} & \overline{\mu_L} & \overline{\tau_L} \end{pmatrix} \gamma^\mu \left[1 - \frac{\sin^4 \phi}{x} + \frac{\sin^2 \phi}{x} L_e^\dagger G L_e \right] \begin{pmatrix} \nu_{eL} \\ \nu_{\mu L} \\ \nu_{\tau L} \end{pmatrix} W_\mu^- + h.c.,$$

$$\frac{e}{\sqrt{2} \sin \theta} \begin{pmatrix} \overline{e_L} & \overline{\mu_L} & \overline{\tau_L} \end{pmatrix} \gamma^\mu \left[-\frac{\sin \phi}{\cos \phi} - \frac{\sin^3 \phi \cos \phi}{x \cos^2 \theta} + \frac{L_e^\dagger G L_e}{\sin \phi \cos \phi} \right] \begin{pmatrix} \nu_{eL} \\ \nu_{\mu L} \\ \nu_{\tau L} \end{pmatrix} W_\mu'^- + h.c. \quad (15)$$

Similarly, for the quark sector we introduce the unitary matrices L_u and L_d . In terms of the mass eigenstates one finds the following interaction terms:

$$\frac{e}{2 \sin \theta \cos \theta} \begin{pmatrix} \overline{u_L} & \overline{c_L} & \overline{t_L} \end{pmatrix} \gamma^\mu \left[1 - \frac{4}{3} \sin^2 \theta - \frac{\sin^4 \phi}{x} + \frac{\sin^2 \phi}{x} L_u^\dagger G L_u \right] \begin{pmatrix} u_L \\ c_L \\ t_L \end{pmatrix} Z_\mu,$$

$$\frac{e}{2 \sin \theta \cos \theta} \begin{pmatrix} \overline{d_L} & \overline{s_L} & \overline{b_L} \end{pmatrix} \gamma^\mu \left[-1 + \frac{2}{3} \sin^2 \theta + \frac{\sin^4 \phi}{x} - \frac{\sin^2 \phi}{x} L_d^\dagger G L_d \right] \begin{pmatrix} d_L \\ s_L \\ b_L \end{pmatrix} Z_\mu,$$

$$\frac{e}{2 \sin \theta} \begin{pmatrix} \overline{u_L} & \overline{c_L} & \overline{t_L} \end{pmatrix} \gamma^\mu \left[-\frac{\sin \phi}{\cos \phi} - \frac{\sin^3 \phi \cos \phi}{x \cos^2 \theta} (1 - \frac{4}{3} \sin^2 \theta) + \frac{L_u^\dagger G L_u}{\sin \phi \cos \phi} \right] \begin{pmatrix} u_L \\ c_L \\ t_L \end{pmatrix} Z'_\mu,$$

$$\frac{e}{2 \sin \theta} \begin{pmatrix} \overline{d_L} & \overline{s_L} & \overline{b_L} \end{pmatrix} \gamma^\mu \left[\frac{\sin \phi}{\cos \phi} + \frac{\sin^3 \phi \cos \phi}{x \cos^2 \theta} (1 - \frac{2}{3} \sin^2 \theta) - \frac{L_d^\dagger G L_d}{\sin \phi \cos \phi} \right] \begin{pmatrix} d_L \\ s_L \\ b_L \end{pmatrix} Z'_\mu,$$

$$\begin{aligned}
& \frac{e}{\sqrt{2}\sin\theta} \begin{pmatrix} \overline{u}_L & \overline{c}_L & \overline{t}_L \end{pmatrix} \gamma^\mu \left[\left(1 - \frac{\sin^4\phi}{x}\right) L_u^\dagger L_d + \frac{\sin^2\phi}{x} L_u^\dagger G L_d \right] \begin{pmatrix} d_L \\ s_L \\ b_L \end{pmatrix} W_\mu^+ + h.c., \\
& \frac{e}{\sqrt{2}\sin\theta} \begin{pmatrix} \overline{u}_L & \overline{c}_L & \overline{t}_L \end{pmatrix} \gamma^\mu \left[\left(-\frac{\sin\phi}{\cos\phi} - \frac{\sin^3\phi \cos\phi}{x} \right) L_u^\dagger L_d + \frac{L_u^\dagger G L_d}{\sin\phi \cos\phi} \right] \begin{pmatrix} d_L \\ s_L \\ b_L \end{pmatrix} W_\mu'^+ + h.c.
\end{aligned} \tag{16}$$

The right-handed fermion couplings to the neutral gauge bosons Z and Z' are, respectively, given by

$$\begin{aligned}
& \frac{e}{2\sin\theta\cos\theta} (-2Q\sin^2\theta), \\
& \frac{e}{2\sin\theta} \left(2Q\sin^2\theta \frac{\sin^3\phi \cos\phi}{x\cos^2\theta} \right).
\end{aligned} \tag{17}$$

The fermion couplings to the photon are the usual electromagnetic couplings. As shown above, it is evident that if $g_h > g_l$, then the heavy gauge bosons would couple strongly to the third generation and weakly to the first two generations, and vice versa.

For the charged-current interactions in the quark sector, one observes that in the case of ignoring the new physics effect, quark mixing is described by a unitary matrix $V = L_u^\dagger L_d$ which is identified as the usual Cabibbo-Kobayashi-Maskawa (CKM) mixing matrix. With the inclusion of new physics, the mixing acquires an additional contribution proportional to $\sin^2\phi/x$, with

$$L_u^\dagger G L_d = L_u^\dagger L_d L_d^\dagger G L_d = V L_d^\dagger G L_d = L_u^\dagger G L_u V. \tag{18}$$

Therefore, we would expect the extracted values of the CKM matrix elements to be slightly modified due to the new contributions of the model.

In this model, lepton mixing is an exciting possibility. Needless to say, there are already significant constraints on lepton universality and lepton number violation from the low energy data. As an example is the almost vanishing decay width $\Gamma_{\mu^- \rightarrow e^- e^+ e^-}$ which severely suppresses any possible mixing between the first and second lepton generations. Similarly, the experimental limit on the decay width $\Gamma_{\mu^- \rightarrow e^- \gamma}$ does not favor such a mixing. Since the other lepton number violation processes, especially those involving the third family, are not as well constrained as $\mu \rightarrow eee$ and $\mu \rightarrow e \gamma$ [10], it is still interesting to explore such a possibility. Furthermore, FCNCs can exist in the neutrino sector in spite that the neutrinos are massless, that may induce an interesting effect to the neutrino oscillation phenomena. As to be shown later, FCNCs are unavoidable in the quark sector of the model, which can lead to appreciable effects that can be verified or ruled out by future data on Kaon and B physics.

In the following sections, we discuss the effect of the new physics predicted by this model to low energy experiments, and derive the constraints on the parameter space of the model from the present data. Using the latest LEP/SLC data we update our

previous analysis in Ref. [5]. For completeness, we also study the constraints from current data on a model in which only the top and bottom doublet has a different $SU(2)$ gauge interaction, which is another possible model of top quark interactions. Furthermore, we shall systematically include all the low energy data from Tau, Kaon, and B physics, and identify a few interesting observables that can be sensitive to this type of new physics. We have also examined the one-loop contribution to the K^0 - \overline{K}^0 , B^0 - \overline{B}^0 mixing, and to the branching ratio of $b \rightarrow s\gamma$.

3 Constraints Imposed by Z -Pole Data

In the SM, the parameters α , G_F , and M_Z are determined through three experimental measurements, e.g., e - p scattering, μ decay, and Z peak at LEP/SLC, respectively. In this model, two additional parameters enter through the gauge sector. These two parameters can be taken as x and $\sin^2 \phi$ (or equivalently, the heavy gauge boson mass $M_{Z'}$ and its decay width $\Gamma_{Z'}$). Similar to the SM case, it is necessary to fix the input parameters α , G_F , M_Z , $\sin^2 \phi$, and x in this model to make prediction and compare with experimental data. The first three parameters can be fixed in the same way as the SM, and the last two parameters, $\sin^2 \phi$ and x , will be constrained through available data. Because of the symmetry-breaking pattern, the electromagnetic coupling α coincides with the SM value. To fix the weak coupling constant, we use the μ -lifetime to define G_F . We calculate the μ -decay width in this model by including the W and W' contributions. We find that, as to be discussed later, $G_F = G_F^{\text{SM}}$ (equivalently $v = v^{\text{SM}}$) as long as one demands no mixing between the first and second lepton families [5]. Finally, we define M_Z using the Z peak at LEP/SLC, i.e., $M_Z = M_Z^{\text{SM}}$.

In Ref. [5] we studied the constraints imposed by the already existed LEP and SLC data, we found that the lower bound on the heavy gauge boson mass was $M_{Z'} \simeq 1.3$ TeV at the 3σ level. The lower limit on $M_{Z'}$ was established for small values of $\sin^2 \phi$, for larger values of $\sin^2 \phi$ the lower bound on $M_{Z'}$ is larger. Since the Z -pole physics program at LEP has completed, it is worthwhile to update our previous analysis using the most recent data. Following Ref. [5], we calculate the changes in the relevant physical observables relative to their SM values to leading order in $1/x$, i.e.,

$$O = O^{\text{SM}} (1 + \delta O) , \quad (19)$$

where O^{SM} is the SM prediction (including the one-loop SM correction) for the observable O , and δO represents the new physics effect to leading order in $1/x$. We list the calculated observables as follows:

$$\Gamma_Z = \Gamma_Z^{\text{SM}} \left(1 + \frac{1}{x} [-0.896 \sin^4 \phi + 0.588 \sin^2 \phi] \right) ,$$

$$R_e = R_e^{\text{SM}} \left(1 + \frac{1}{x} [0.0794 \sin^4 \phi + 0.549 \sin^2 \phi] \right) ,$$

$$R_\mu = R_\mu^{\text{SM}} \left(1 + \frac{1}{x} \left[0.0794 \sin^4 \phi + 0.549 \sin^2 \phi - 2.139 \sin^2 \beta \sin^2 \phi \right] \right) ,$$

$$R_\tau = R_\tau^{\text{SM}} \left(1 + \frac{1}{x} \left[0.0794 \sin^4 \phi + 0.549 \sin^2 \phi - 2.139 \cos^2 \beta \sin^2 \phi \right] \right) ,$$

$$A_{FB}^e = (A_{FB}^e)^{\text{SM}} \left(1 + \frac{1}{x} \left[10.44 \sin^4 \phi \right] \right) ,$$

$$A_{FB}^\mu = (A_{FB}^\mu)^{\text{SM}} \left(1 + \frac{1}{x} \left[10.44 \sin^4 \phi + 12.14 \sin^2 \beta \sin^2 \phi \right] \right) ,$$

$$A_{FB}^\tau = (A_{FB}^\tau)^{\text{SM}} \left(1 + \frac{1}{x} \left[10.44 \sin^4 \phi + 12.14 \cos^2 \beta \sin^2 \phi \right] \right) ,$$

$$A_e = A_e^{\text{SM}} \left(1 + \frac{1}{x} \left[5.22 \sin^4 \phi \right] \right) ,$$

$$A_\tau = A_\tau^{\text{SM}} \left(1 + \frac{1}{x} \left[5.22 \sin^4 \phi + 12.14 \cos^2 \beta \sin^2 \phi \right] \right) ,$$

$$\sigma_h^0 = (\sigma_h^0)^{\text{SM}} \left(1 + \frac{1}{x} \left[-0.01 \sin^4 \phi - 0.628 \sin^2 \phi \right] \right) ,$$

$$M_W = M_W^{\text{SM}} \left(1 + \frac{1}{x} \left[1 + 0.215 \sin^4 \phi \right] \right) ,$$

$$R_b = R_b^{\text{SM}} \left(1 + \frac{1}{x} \left[-0.015 \sin^4 \phi + 1.739 \sin^2 \phi \right] \right) ,$$

$$R_c = R_c^{\text{SM}} \left(1 + \frac{1}{x} \left[0.038 \sin^4 \phi - 0.549 \sin^2 \phi \right] \right) ,$$

$$A_b = A_b^{\text{SM}} \left(1 + \frac{1}{x} \left[0.068 \sin^4 \phi + 0.157 \sin^2 \phi \right] \right) ,$$

$$A_c = A_c^{\text{SM}} \left(1 + \frac{1}{x} \left[0.514 \sin^4 \phi \right] \right) ,$$

$$A_{FB}^c = (A_{FB}^c)^{\text{SM}} \left(1 + \frac{1}{x} \left[5.734 \sin^4 \phi \right] \right) , \tag{20}$$

where β is the lepton mixing angle, which will be discussed in the following sections. In this analysis we do not include the measurement of A_{LR} at SLC and the measurement of A_{FB}^b at LEP. The quantity A_{LR} in the proposed model is identical to A_e , therefore, this model cannot explain the discrepancy between the SLC measurement $A_{LR} = 0.1547 \pm 0.0032$ and the LEP measurement $A_e = 0.1399 \pm 0.0073$ [9]. The SM predicts $A_{FB}^b = 0.1040$, which is more than 2σ above the LEP measurement $A_{FB}^b = 0.0984 \pm 0.0024$ [9]. The new contribution in this model to A_{FB}^b can be found as

$$A_{FB}^b = (A_{FB}^b)^{\text{SM}} \left(1 + \frac{1}{x} \left[5.287 \sin^4 \phi + 0.157 \sin^2 \phi \right] \right). \quad (21)$$

which is positive and thus it worsens the discrepancy with LEP data. Therefore, we cannot accommodate either A_{LR} or A_{FB}^b in this model at the 2σ level.

Following Ref. [5] and using the most recent LEP and SLC measurements [9], shown in Table 1 (which includes the total width of the Z boson Γ_Z , R_e , R_μ , R_τ , the vector g_{Ve} and the axial-vector g_{Ae} couplings of the electron, the ratios $g_{V(\mu,\tau)}/g_{Ve}$, $g_{A(\mu,\tau)}/g_{Ae}$, A_{FB}^e , A_{FB}^μ , A_{FB}^τ , A_e , A_τ , M_W , the hadronic cross section σ_h^0 , R_b , R_c , A_b , A_c , and A_{FB}^c), we update the allowed values of $\sin^2 \phi$ and x at the 2σ level. The SM prediction for the observables listed in Table 1 is given for $m_t = 175$ GeV, $\alpha_s = 0.118$, $m_H = 100$ GeV, $1/\alpha(M_Z^2) = 128.75$, $M_Z = 91.187$ GeV, and $G_F = 1.16637 \times 10^{-5} \text{ GeV}^{-2}$ [11].

In Figure 1 (solid curve) we show the minimal Z' mass as a function of $\sin^2 \phi$ at the 2σ level for the case that there is no mixing in the lepton sector. We find that $M_{Z'}$ is constrained to be larger than about 1.9 TeV. (At the 3σ level, this corresponds to about 1.4 TeV.) In Figure 2 (solid curve), we show the constraint for the quantity x as a function of $\sin^2 \phi$. We find that x can be as small as 20 for the smallest value of $\sin^2 \phi$ ($= 0.04$), and it increases as $\sin^2 \phi$ increases. For example, $x > 90$ for $\sin^2 \phi > 0.2$. Furthermore, the quantity $\sin^2 \phi/x$ is constrained by data to be less than about 2×10^{-3} for a large range of $\sin^2 \phi$.

We find the most important factor in constraining the free parameters of the model is the breakdown of the universality property of the gauge boson couplings to leptons. The Z -pole observable that imposes the most stringent constraint on the model is R_τ , which is the ratio of the partial decay widths of $Z \rightarrow \tau^+ \tau^-$ and the hadronic modes. The measurement of Γ_Z also plays an important role secondary to R_τ , especially for small $\sin^2 \phi$, due to the high precision of data. It is interesting to note that, as shown in Figure 1 (dotted curve), without including the leptonic observables from the Z -pole data, i.e., only including M_W , R_b , R_c , A_b , A_c , and A_{FB}^c , the bounds on $M_{Z'}$ is about 900 GeV at the 2σ level. Also, Figure 2 (dotted curve), shows that $x > 5$ for $\sin^2 \phi = 0.04$ and $x > 24$ for $\sin^2 \phi > 0.2$. In this case, the important constraint is coming from the measurement of R_b . The last bound is relevant for models in which only the top and bottom doublet has a different $SU(2)$ gauge interaction. In Table 1, we also show the predictions of this model for the Z -pole observables with three choices of the parameters x , $\sin^2 \phi$, and $\sin^2 \beta$.

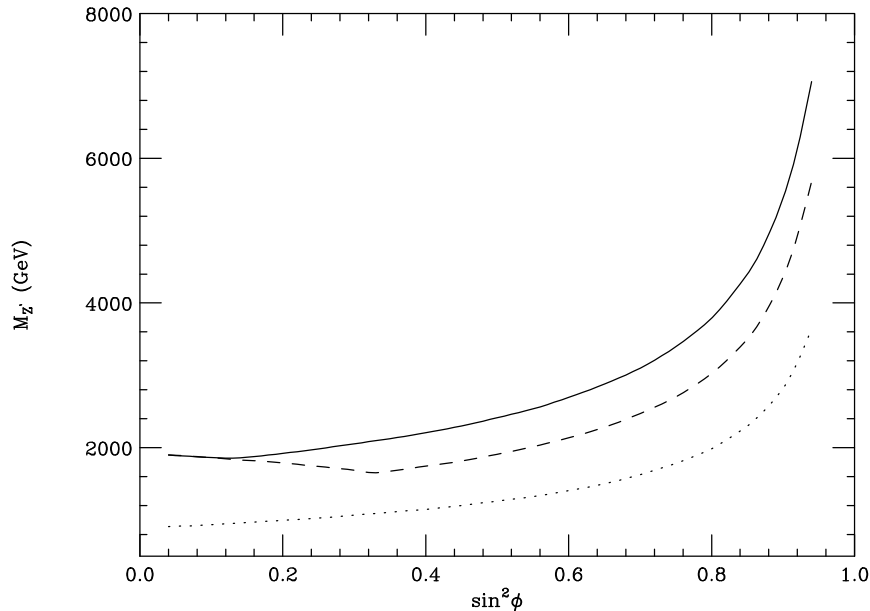


Figure 1: The lower bound on the heavy Z' mass as a function of $\sin^2 \phi$ at the 2σ level. Solid curve: including all Z -pole data and assuming no lepton mixing. Dashed curve: including all Z -pole data and assuming maximal lepton mixing ($\sin^2 \beta = 0.5$). Dotted curve: only including the hadronic measurements in the fit and assuming no lepton mixing.

4 Low-Energy Constraints

Even though the Z -pole data already impose significant constraints, this model has a rich structure that can be further examined at much lower energy scales. In the following sections, we would like to examine those constraints obtained from the low-energy hadronic, leptonic, and semi-leptonic data. We will concentrate on the very low-energy regime, i.e., physics at zero-momentum transfer, and examine whether the parameters of the model can be better constrained than those imposed by LEP and SLC data.

To study the low-energy region, it is necessary to understand the form of the four-fermion current-current interaction at zero-momentum transfer. The four-fermion charged-current weak interactions are given by [5, 12]

$$\frac{2}{v^2}(j_l^\pm + j_h^\pm)^2 + \frac{2}{u^2}j_h^+ j_h^- . \quad (22)$$

The first term refers to the SM contribution, while the second term expresses the new contribution to the order $1/u^2$. The charged current j_l^\pm refers to the first two fermion generations, while j_h^\pm refers to the third generation. For example, for the lepton sector, $j_h^+ = \overline{\tau_L} \gamma_\mu \nu_{\tau_L}$. We note that in the above formula, the charged currents j_h^\pm are written in terms of the weak eigenstates τ_L and ν_{τ_L} and not the mass eigenstates.

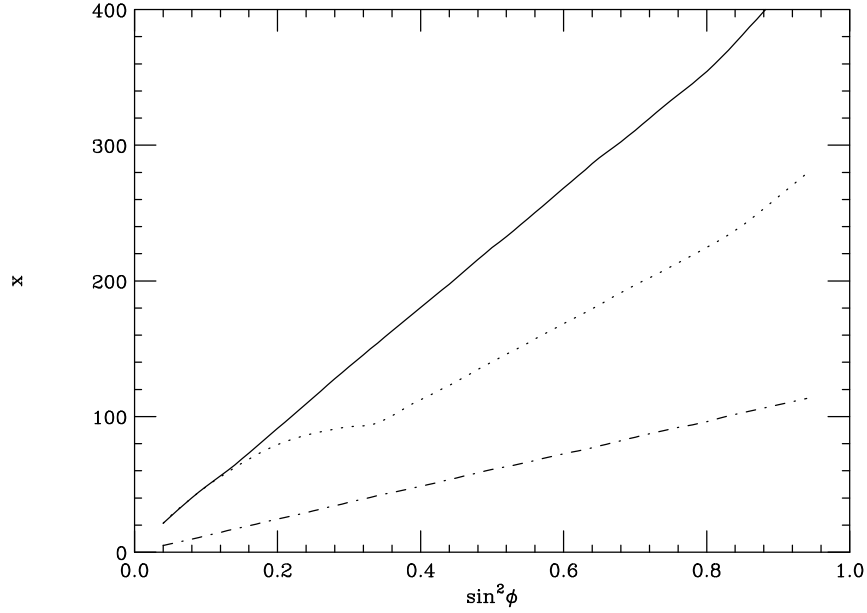


Figure 2: The lower bound on the parameter x as a function of $\sin^2 \phi$ for the 2σ level. Solid curve: including all Z -pole data and assuming no lepton mixing. Dashed curve: including all Z -pole data and assuming maximal lepton mixing ($\sin^2 \beta = 0.5$). Dotted curve: only including the hadronic measurements in the fit and assuming no lepton mixing.

Similarly, the neutral-current four-fermion interactions are given by [5, 12]

$$\frac{4}{v^2}(j_l^3 + j_h^3 - \sin^2 \theta j_{\text{em}})^2 + \frac{4}{u^2}(j_h^3 - \sin^2 \phi \sin^2 \theta j_{\text{em}})^2, \quad (23)$$

where, $j_{l,h}^3$ refers to the left-handed $T_{l,h}^3$ currents, while j_{em} represents the full electromagnetic current of the three families. The first term refers to the SM contribution while the second one represents the extra contribution. For example, for the lepton sector,

$$j_h^3 = \overline{\tau_L} \gamma_\mu \left(\frac{-1}{2} \right) \tau_L + \overline{\nu_{\tau L}} \gamma_\mu \left(\frac{1}{2} \right) \nu_{\tau L}, \quad (24)$$

and

$$j_{\text{em}} = \overline{e} \gamma_\mu (-1) e + \overline{\mu} \gamma_\mu (-1) \mu + \overline{\tau} \gamma_\mu (-1) \tau, \quad (25)$$

in terms of the weak eigenstates.

For clarity, we shall separately discuss below the effects from the lepton and quark sectors to the lepton number violation phenomena, as well as the kaon and bottom physics.

5 The Lepton Sector

As previously mentioned, lepton mixing is an interesting feature of this model. However, because of the almost null measurement of $\mu^- \rightarrow e^- e^+ e^-$ and $\mu^- \rightarrow e^- \gamma$, we expect the mixing between the first and second lepton families to be highly suppressed. Nevertheless, fermion mixing may be large between the third family and the first or second family. To clarify this point, we write the unitary matrix L_e , which is introduced to diagonalize the mass matrix M_e , in the general form

$$L_e = \begin{pmatrix} L_{11} & L_{12} & L_{13} \\ L_{21} & L_{22} & L_{23} \\ L_{31} & L_{32} & L_{33} \end{pmatrix}. \quad (26)$$

It is easy to show that

$$L_e^\dagger G L_e = \begin{pmatrix} |L_{31}|^2 & L_{31}^* L_{32} & L_{31}^* L_{33} \\ L_{31} L_{32}^* & |L_{32}|^2 & L_{32}^* L_{33} \\ L_{31} L_{33}^* & L_{32} L_{33}^* & |L_{33}|^2 \end{pmatrix}. \quad (27)$$

Thus, leptonic FCNC dynamics only depends on the third row of the mixing matrix L_e . In other words, we can only probe the third row of the unitary matrix L_e through the leptonic FCNC processes.

Using the expression for the four-fermion neutral-current interaction, a direct calculation of the decay width $\mu \rightarrow eee$ yields

$$\text{Br}(\mu \rightarrow eee) = \frac{|L_{31}|^2 |L_{32}|^2}{4x^2} \left((|L_{31}|^2 - 2 \sin^2 \phi \sin^2 \theta)^2 + 4 \sin^4 \phi \sin^4 \theta \right). \quad (28)$$

Notice that the partial decay width of $\mu \rightarrow eee$ is already of order $1/x^2$. Therefore, to keep the leading contribution of order $1/x^2$, we set the total decay width, used in the above equation, to be the SM value. The above branching ratio has to be compared with the very stringent limit set by data which is less than 10^{-12} [10]. Thus, a severe constraint on the following combination is established:

$$\frac{|L_{31}|^2 |L_{32}|^2 \sin^4 \phi}{x^2} \lesssim 1.6 \times 10^{-11}. \quad (29)$$

As shown in the previous section, the Z -pole observables bound the quantity of $\sin^2 \phi/x$ to be less than 2×10^{-3} . Therefore, taking $\sin^2 \phi/x \sim 2 \times 10^{-3}$, we get

$$|L_{31}|^2 |L_{32}|^2 < 4 \times 10^{-6}. \quad (30)$$

Another process to consider is $\mu \rightarrow e \gamma$, which can only occur via loop correction in this model. The experimental limit on this branching ratio is found to be less than 4.9×10^{-11} [10]. A one-loop calculation of the branching ratio in the model yields

$$\text{Br}(\mu \rightarrow e \gamma) \simeq 8.7 \times 10^{-4} \frac{|L_{31}|^2 |L_{32}|^2}{x^2} (1 + 1.2 \sin^2 \phi + 1.2 \sin^4 \phi), \quad (31)$$

which implies

$$\frac{|L_{31}|^2|L_{32}|^2}{x^2} < 5.6 \times 10^{-8} \quad (32)$$

when compared with data. For the smallest possible value of $x(\sim 20)$ allowed by Z -pole data, the above constraint yields

$$|L_{31}|^2|L_{32}|^2 \lesssim 2.2 \times 10^{-5}, \quad (33)$$

which is weaker (by a factor of 5) than the one imposed by the measurement of $\mu \rightarrow eee$. Other limits on FCNC processes, such as $\tau \rightarrow eee$, $\tau \rightarrow \mu\mu\mu$, $\tau \rightarrow ee\mu$, are not as severe as the ones mentioned above. (Their branching ratios are typically bounded from above at the order of 10^{-6} [10].)

The above constraints on the elements of the lepton mixing matrix L_e can be automatically satisfied if $L_{31} = 0$ and/or $L_{32} = 0$, which means there is no mixing between the third family and the first and/or the second family leptons. Consequently, with this choice, this model predicts no transition between μ and e leptons. Although both cases of lepton mixing are allowed, it is more natural to assume the mixing strength between leptons to be directly related to their masses. If so, one would expect the mixing between the second and third families to be more significant than the first and third families. Hence, in the following discussion, we will assume that leptonic mixing is only allowed between the second and third families (i.e., we set $L_{31} = 0$).

The lepton-mixing matrix has the form $L_e^\dagger G L_e$, given in Eq. (27), where the matrix G is defined in Eq. (14). Using unitarity of L_e and taking $L_{31} = 0$, we have $|L_{32}|^2 + |L_{33}|^2 = 1$. Therefore, the mixing matrix between the second and third lepton families can be simply expressed in terms of a one free real parameter, and the 2×2 mixing matrix can be written as

$$\begin{pmatrix} \sin^2 \beta & \cos \beta \sin \beta \\ \cos \beta \sin \beta & \cos^2 \beta \end{pmatrix}, \quad (34)$$

where $\sin \beta$ is a free parameter of the model for describing the mixing between the second and third lepton families. The phases in the matrix $L_e^\dagger G L_e$ can be simply absorbed in the definitions of the lepton fields. It is easy to see that if there is no mixing among leptons, then all the leptonic decay rates are identical to the SM, and τ lifetime is not modified. (This also explains why $G_F = G_F^{\text{SM}}$ from the μ -decay if there is no mixing between the first and second lepton families.) If the lepton mixing involves the third family, then the lifetime of the τ lepton will be modified.

At this stage it is relevant to return back to the LEP and SLC data and study the new constraints on the model if a mixing between μ and τ is allowed. In this case we also need to include the limit on the branching ratio of $Z \rightarrow \mu\tau$, which is found to be less than 1.7×10^{-5} at the 2σ level [10]. In Figure 1 (dashed curve), we depict the new constraints on $\sin^2 \phi$ and $M_{Z'}$ for the case of a maximal possible mixing, i.e., $\sin^2 \beta = 0.5$. We find that the lower limit on the heavy mass is reduced to $M_{Z'} \approx 1.7$ TeV, which is slightly lower than that for the case of no mixing (≈ 1.9

TeV). The reason for this lower bound is due to the reduced non-universal effect in R_τ . In Figure 2 (dashed curve) we show the new constraint on x , assuming the maximal lepton mixing. We find that for the smallest value of $\sin^2 \phi = 0.04$, the value of x can be as low as 20. For $\sin^2 \phi = 0.2$, $x > 80$. The quantity $\sin^2 \phi/x$ is found to be less than about 0.3%. It is interesting to notice that the lower bound $x = 20$ is the same for both cases of $\sin^2 \beta = 0$ and $\sin^2 \beta = 0.5$. The reason is that for small values of $\sin^2 \phi < 0.2$, the measurement Γ_Z , which is independent of the mixing angle $\sin^2 \beta$, plays the important rule in constraining the parameter x . In Table 1, we give a few predictions of this model with various $\sin^2 \beta$ for the Z -pole observables.

Next, we examine the other interesting low-energy leptonic processes and ask whether we can learn more about the proposed model. We start by examining the decay process $\tau \rightarrow \mu \bar{\nu}_\mu \nu_\tau$. In this model, both the charged and neutral currents contribute to the decay width $\Gamma(\tau^- \rightarrow \mu^- \bar{\nu}_\mu \nu_\tau)$. Adding both contributions, we find

$$\Gamma(\tau^- \rightarrow \mu^- \bar{\nu}_\mu \nu_\tau) = \Gamma^{\text{SM}}(\tau^- \rightarrow \mu^- \bar{\nu}_\mu \nu_\tau) \left(1 + \frac{3 \cos^2 \beta \sin^2 \beta}{x}\right). \quad (35)$$

The only modification to the total decay width, at the order of $1/x$, is coming from the partial decay width $\Gamma(\tau^- \rightarrow \mu^- \bar{\nu}_\mu \nu_\tau)$. The partial decay width $\Gamma(\tau^- \rightarrow e^- \bar{\nu}_e \nu_\tau)$ is not modified because of the assumption of no $\tau \leftrightarrow e$ mixing. The ratio $\Gamma(\tau^- \rightarrow \mu^- \bar{\nu}_\mu \nu_\tau) / \Gamma(\tau^- \rightarrow e^- \bar{\nu}_e \nu_\tau)$, can be written as

$$\frac{\Gamma(\tau^- \rightarrow \mu^- \bar{\nu}_\mu \nu_\tau)}{\Gamma(\tau^- \rightarrow e^- \bar{\nu}_e \nu_\tau)} = \frac{\text{Br}(\tau^- \rightarrow \mu^- \bar{\nu}_\mu \nu_\tau)}{\text{Br}(\tau^- \rightarrow e^- \bar{\nu}_e \nu_\tau)} = f(m_\mu/m_\tau) \left(1 + \frac{3 \cos^2 \beta \sin^2 \beta}{x}\right), \quad (36)$$

where $f(m_\mu/m_\tau)$ is a phase factor given by [13]

$$f(y) = 1 - 8y^2 + 8y^6 - y^8 - 24y^4 \ln(y). \quad (37)$$

Hence, an increase by a factor of $3 \cos^2 \beta \sin^2 \beta/x$ is expected in the above ratio.

The experimental measurement of $\Gamma(\tau^- \rightarrow \mu^- \bar{\nu}_\mu \nu_\tau) / \Gamma(\tau^- \rightarrow e^- \bar{\nu}_e \nu_\tau)$ can directly constrain the quantity $\cos^2 \beta \sin^2 \beta/x$. As shown by the Particle Data Group (PDG) [10], for the ratio $\Gamma(\tau^- \rightarrow \mu^- \bar{\nu}_\mu \nu_\tau) / \Gamma(\tau^- \rightarrow e^- \bar{\nu}_e \nu_\tau)$, the average of the available experimental data yields 0.978 ± 0.011 while the result of a global fit gives 0.976 ± 0.006 . In this model, new decay channels for the τ lepton can occur, e.g., $\tau \rightarrow \mu \mu \mu$ and $\tau \rightarrow \mu \gamma$. However, as to be discussed below, their decay widths can only be modified at the order $1/x^2$. Thus, to the order $1/x$, we can use both data, the average and the fit results, to constrain the parameter x . Using the PDG data average and assuming a maximal lepton mixing $\sin^2 \beta = 0.5$, we find $x > 27$ at the 2σ confidence level. On the other hand, using the PDG fit result we find $x > 48$. The difference in the x range, 27 to 48 can then be interpreted as the theoretical error in our model.

For a lepton mixing angle $\sin^2 \beta$ smaller than 0.5, the constraint on the parameter x is more relaxed. If there is no lepton mixing at all, then the decay width of $\tau^- \rightarrow \mu^- \bar{\nu}_\mu \nu_\tau$ is not modified as compared with the SM prediction. Since this decay width is independent of the parameter $\sin^2 \phi$ (gauge coupling) and the only dependence besides lepton mixing is the parameter x (the ratio of the two symmetry-breaking scales of

the gauge group), this measurement imposes a direct and significant constraint on x for a non-vanishing $\sin^2 \beta$.

Another interesting process for testing this model is to detect $\tau \rightarrow \mu\mu\mu$. One can show that³, keeping the leading contribution in $1/x$,

$$\frac{\text{Br}(\tau^- \rightarrow \mu^- \mu^- \mu^+)}{\text{Br}(\tau^- \rightarrow \mu^- \nu_\tau \bar{\nu}_\mu)} = \frac{\sin^2 \beta \cos^2 \beta}{4x^2} \left(\sin^4 \beta - 4 \sin^2 \beta \sin^2 \theta \sin^2 \phi + 8 \sin^4 \phi \sin^4 \theta \right). \quad (38)$$

This decay width will also impose a direct constraint on the parameters of the model. For $\sin^2 \beta = 0.5$ and $\sin^2 \phi = 0.04$, the predicted branching ratio is

$$\text{Br}(\tau^- \rightarrow \mu^- \mu^- \mu^+) \simeq \frac{0.0025}{x^2}. \quad (39)$$

If we compare this effect with data which is found to be less than 1.9×10^{-6} [10], the parameter x is constrained to be above 37, which is consistent with the constraint ($x > 27 \sim 48$) derived from the measurement of $\text{Br}(\tau \rightarrow \mu \bar{\nu}_\mu \nu_\tau) / \text{Br}(\tau \rightarrow e \bar{\nu}_e \nu_\tau)$.

Other processes to consider is the lepton number violation process $\tau \rightarrow \mu \gamma$, which can only occur in this model at the loop level. For this process, up to the order $1/x$, there are four diagrams which contribute to the one-loop amplitude, Two of those diagrams involve either two W or two W' exchange. The other two diagrams involve Z or Z' exchange (due to FCNC). A detailed calculation of the branching ratio yields

$$\text{Br}(\tau \rightarrow \mu \gamma) \simeq 1.5 \times 10^{-4} \frac{\sin^2 \beta \cos^2 \beta}{x^2} (1 + 1.2 \sin^2 \phi + 1.2 \sin^4 \phi). \quad (40)$$

This result has to be compared with the limit imposed by data (less than 4.2×10^{-6} [10]). For a maximal possible mixing effect, the present limit on the above branching ratio is not of any significance in constraining the values of x (> 3).

The final leptonic observable we consider is the anomalous magnetic dipole moment of the muon, $a_\mu = \frac{1}{2}(g - 2)_\mu$. A precise measurement of a_μ is underway at Brookhaven National Laboratory (BNL) with a perspective goal [14] of

$$\Delta a_\mu^{\text{exp.}} = 4.0 \times 10^{-10}. \quad (41)$$

At this level of accuracy, higher order electroweak corrections become important and new physics at higher energy scales can be probed.

The one-loop electroweak contribution to a_μ as predicted by the SM is [15]

$$a_\mu^{\text{weak}} \approx 19.5 \times 10^{-10}. \quad (42)$$

In our proposed model the one-loop electroweak contribution is modified due to the modified couplings and the new heavy gauge bosons. We calculate the new contribution to a_μ at the one-loop level. We find the new contribution to the anomalous magnetic dipole moment to be

$$a_\mu^{\text{new}} \approx a_\mu^{\text{weak}} \frac{\sin^2 \beta}{x}. \quad (43)$$

³ Our prediction for $\text{Br}(\tau \rightarrow \mu\mu\mu)$ is slightly different from that in Ref. [7].

Using the Z -pole constraints, for a maximal mixing, $\sin^2 \beta = 0.5$ and $x \geq 20$ we conclude that the new contribution does not exceed the level of 0.5×10^{-10} . Therefore, the predicted new effect to a_μ is too small to be detected even at the perspective precision at BNL.

In conclusion, assuming the third family lepton does not mix with the first family lepton, then the partial decay widths of $\mu \rightarrow eee$, $\mu \rightarrow e\gamma$, and $\tau \rightarrow e\bar{\nu}_e\nu_\tau$ are not modified. However, for the maximal mixing case, the measurement of the ratio $\Gamma(\tau \rightarrow \mu\bar{\nu}_\mu\nu_\tau)/\Gamma(\tau \rightarrow e\bar{\nu}_e\nu_\tau)$ constrain the parameter $x > 27 \sim 48$. Also the lepton number violation process $\tau \rightarrow \mu\mu\mu$ provides the constraint $x > 37$ consistent with the above measurement. Therefore, the above two measurements give a stronger constraint than the Z -pole data for $\sin^2 \phi < 0.1$ (cf. Figure 2). On the other hand, given the current experimental data, the decay process $\tau \rightarrow \mu\gamma$ and the anomalous magnetic dipole moment of the muon have not yet played a significant role in constraining the model. Nevertheless, if the above discussed processes can be measured to a better accuracy in future experiments, they can further test the proposed model. In discussing the predictions of our model to other low-energy processes we will use the range $x \geq 20$ for $\sin^2 \beta = 0.0$, and $x \geq 48$ for $\sin^2 \beta = 0.5$.

6 The Quark Sector

The quark sector has a far more rich structure than the lepton sector in this model. To completely describe the interactions of gauge bosons and quarks, it requires two mixing matrices L_u and L_d because both the up- and down-type quarks are massive. As noted in Eq. (16) the neutral-current mixing matrices ($L_u^\dagger GL_u$ and $L_d^\dagger GL_d$) are related to the charged-current mixing matrix ($L_u^\dagger L_d$). Because of the experimental evidence of the CKM matrix in charged currents, FCNCs must occur in the interaction of quarks to gauge bosons.

First we make the following observation. Assume neither up- or down-type quark sectors has FCNC, i.e., assume L_u (and L_d) has the general form

$$L_u = \begin{pmatrix} u_{11} & u_{12} & 0 \\ u_{21} & u_{22} & 0 \\ 0 & 0 & u_{33} \end{pmatrix}. \quad (44)$$

It is straight forward to show that $L_u^\dagger GL_u = L_d^\dagger GL_d = G$ and that the charged-current mixing matrix $V = L_u^\dagger L_d$ has the same general form as L_u and L_d . This means that V will only mix the first and second generation, i.e., the CKM matrix is a 2×2 matrix. Therefore, unless we assume the existence of FCNCs in the quark sector, this model cannot explain some observed decay processes, such as $B_d^0 \rightarrow J/\psi(1S) K^0$, in which $b \rightarrow cW^* \rightarrow c\bar{c}s$ whose branching ratio was measured to be $(7.5 \pm 2.1) \times 10^{-4}$ [10]. Hence, FCNCs must exist in the quark sector.

Based on the above observation, FCNC data in the quark sector can be used to further test this model. FCNCs in the quark sector can be realized in three possible ways: (i) in the down-quark sector only, (ii) in the up-quark sector only, and (iii) in

both sectors. All the three possibilities have to confront the large body of existing low-energy data. In the following, we investigate these three possibilities, separately.

6.1 Mixing in the Down-Quark Sector

Here, we consider the case that only down-type quarks can mix, so that $L_u^\dagger G L_u = G$, and $L_d^\dagger G L_d = V^\dagger G V$. In this case, the quark interactions to the gauge bosons are given in Eq. (16) with the above substitutions. Similar to the SM case, the mixing matrix V contains the same number of independent parameters, namely, three real parameters and one phase. Therefore, there is no extra parameter in the quark sector in spite of the new features of the model. This implies that FCNC processes are completely determined by the matrix V in addition to the other two parameters $\sin^2 \phi$ and x . The matrix $V^\dagger G V$ can be explicitly written as

$$V^\dagger G V = \begin{pmatrix} |V_{td}|^2 & V_{ts}V_{td}^* & V_{tb}V_{td}^* \\ V_{td}V_{ts}^* & |V_{ts}|^2 & V_{tb}V_{ts}^* \\ V_{td}V_{tb}^* & V_{ts}V_{tb}^* & |V_{tb}|^2 \end{pmatrix}. \quad (45)$$

It is interesting to notice that the matrix elements of $V^\dagger G V$ are naturally small, so that we generally do not expect large effects in FCNC processes.

6.1.1 Charged-Current Phenomenology

In general, this model predicts new contributions to charged-current processes as well. Under the down-quark mixing scenario, the non-standard contribution to charged-current processes can be written as

$$\frac{2\sqrt{2}G_F}{x} j_h^+ j_h^-, \quad (46)$$

where $j_h^- = \bar{t}_L \gamma_\mu b_L$, written in terms of the weak eigenstates t_L and b_L . Since we assume no FCNCs in the up-type quark sector, the top quark does not mix with the other up-type quarks at tree level. Furthermore, for the low-energy charged-current observables (with momentum transfer q^2 much less than M_Z^2), top quark does not contribute at tree level. Hence, we conclude that under this scenario, no new physics effect to the low-energy charged-current interaction is expected at tree level. Therefore, the values of the CKM matrix elements extracted from low-energy charged-current data coincide with those in the SM.

6.1.2 Neutral-Current Phenomenology

On the contrary, the neutral-current hadronic and semi-leptonic interactions can be modified at tree level for the case of down-type quark mixing. The non-standard contribution to neutral-current processes can be written as

$$\frac{4\sqrt{2}G_F}{x} (j_h^3 - \sin^2 \phi \sin^2 \theta j_{em})^2, \quad (47)$$

where j_h^3 contains $\overline{b_L}\gamma_\mu(-1/2)b_L$, written in terms of the weak eigenstate. In terms of the mass eigenstates, the following currents are generated: $|V_{td}|^2\overline{d_L}\gamma_\mu d_L$, $|V_{ts}|^2\overline{s_L}\gamma_\mu s_L$, $|V_{tb}|^2\overline{b_L}\gamma_\mu b_L$, $V_{td}^*V_{ts}\overline{d_L}\gamma_\mu s_L$, $V_{td}^*V_{tb}\overline{d_L}\gamma_\mu b_L$, and $V_{ts}^*V_{tb}\overline{s_L}\gamma_\mu b_L$, whose effects to low-energy FCNC data are discussed as follows.

The first interesting process to investigate is the K^0 - \overline{K}^0 mixing, whose transition amplitude receives in this model a new contribution at the tree level. Up to the order of $1/x$, it is

$$T = \frac{\sqrt{2}G_F}{x}(V_{td}V_{ts}^*)^2[\overline{s_L}\gamma_\mu d_L][\overline{s_L}\gamma_\mu d_L]. \quad (48)$$

In the SM, ignoring the QCD corrections, the short distance transition amplitude induced from box diagrams for the K^0 - \overline{K}^0 mixing is given by [16, 17]

$$T^{\text{SM}} = \frac{G_F^2 M_W^2}{\pi^2} [\lambda_c^2 S(y_c) + \lambda_t^2 S(y_t) + 2\lambda_c \lambda_t S(y_c, y_t)] [\overline{s_L}\gamma_\mu d_L][\overline{s_L}\gamma_\mu d_L], \quad (49)$$

where, $y_c = m_c^2/M_W^2$, $y_t = m_t^2/M_W^2$, $\lambda_c = V_{cs}^*V_{cd}$, $\lambda_t = V_{ts}^*V_{td}$, and the functions $S(y)$ and $S(y_c, y_t)$ are the Inami-Lim functions [17]:

$$S(y) = y \left[\frac{1}{4} + \frac{9}{4} \frac{1}{1-y} - \frac{3}{2} \frac{1}{(1-y)^2} \right] - \frac{3}{2} \left[\frac{y}{1-y} \right]^3 \ln y, \\ S(y_c, y_t) = -y_c \ln y_c + y_c \left[\frac{y_t^2 - 8y_t + 4}{4(1-y_t)^2} \ln y_t + \frac{3}{4} \frac{y_t}{y_t - 1} \right]. \quad (50)$$

When comparing the non-standard and the SM amplitude, which is proportional to the ΔM ratio, we find approximately

$$\frac{\Delta M}{\Delta M^{\text{SM}}} = \frac{T}{T^{\text{SM}}} \lesssim \frac{4}{x}, \quad (51)$$

in which we have used $m_t = 175$ GeV, $m_c = 1.5$ GeV, $M_W = 80.4$ GeV and all the CKM elements are taken from Refs. [10, 18]. For $x > 20$ (implied by Z -pole data), it would correspond to a change in the transition amplitude by less than about 20%. Although the mass difference between K_L and K_S states has been measured experimentally with a great accuracy (about 0.4%), the theoretical uncertainty in the long distance part of contribution remains to be improved. (Currently, its uncertainty is about 40% to 60% [16].) To use the K^0 - \overline{K}^0 mixing data to further test this model requires a better understanding of the long-distance contribution.

It is well known that the rare decay process $K^+ \rightarrow \pi^+ \nu \overline{\nu}$ is one of the best places to search for new physics. This is because its decay rate has a small theoretical uncertainty, and the long-distance contribution has been estimated to be less than 10^{-3} of the short-distance contribution [19]. Recently, E787 collaboration reported the first observation consistent with this decay rate and obtained $\text{Br}(K^+ \rightarrow \pi^+ \nu \overline{\nu}) = 4.2_{-3.5}^{+9.7} \times 10^{-10}$ [20]. The branching ratio predicted by the SM is $\text{Br}^{\text{SM}}(K^+ \rightarrow \pi^+ \nu \overline{\nu}) = (9.1 \pm 3.8) \times 10^{-11}$, where the error is dominated by the uncertainties of the CKM matrix elements [21].

Since under the scenario considered, this process can occur at the tree level through the flavor-changing neutral current $s \rightarrow d Z \rightarrow d \nu \bar{\nu}$, it can be used to test the model. The expected branching ratio, normalized to the predicted branching ratio for $K^+ \rightarrow \pi^0 e^+ \nu_e$, can be written as

$$\frac{\text{Br}(K^+ \rightarrow \pi^+ \nu \bar{\nu})}{\text{Br}(K^+ \rightarrow \pi^0 e^+ \nu_e)} = \frac{1}{4x^2} \left(\frac{|V_{td}|^2 |V_{ts}|^2}{|V_{us}|^2} \right). \quad (52)$$

It is obvious that the partial decay width of $K^+ \rightarrow \pi^0 e^+ \nu_e$ predicted by this model coincides with the SM prediction at tree level for the undertaken scenario that the third family lepton does not mix with the first family lepton. Therefore, assuming the experimental data $\text{Br}(K^+ \rightarrow \pi^0 e^+ \nu_e) = (4.82 \pm 0.06) \times 10^{-2}$ [10] to be consistent with the model, we can compare the predicted $\text{Br}(K^+ \rightarrow \pi^+ \nu \bar{\nu})$ with the E787 result. After spanning all the allowed values of the CKM elements, we find that

$$\text{Br}(K^+ \rightarrow \pi^+ \nu \bar{\nu}) \lesssim \frac{1.1 \times 10^{-7}}{x^2}, \quad (53)$$

in which we have included all three neutrino species, i.e., $\nu_\mu \bar{\nu}_\mu$, $\nu_\tau \bar{\nu}_\tau$, $\nu_\mu \bar{\nu}_\tau$, and $\nu_\tau \bar{\nu}_\mu$, so that the lepton mixing angle dependence cancel. Comparing this branching ratio with the E787 result, we can set a lower bound $x > 7$ at the 2σ level based on one observed event. For $x > 20$ (as implied by Z -pole data), this branching ratio is smaller than about 3×10^{-10} , which is however larger than the SM prediction by almost an order of magnitude.

The measurement of $\text{Br}(K^+ \rightarrow \pi^+ \nu \bar{\nu})$ is highly valuable in our analysis because it is independent of the parameters $\sin^2 \beta$ and $\sin^2 \phi$. It directly constrains the parameter x independently of the other parameters. Hence, an improvement on the measurement of this branching ratio is very important to test this model.

Similarly, this model predicts non-standard effects for bottom quark physics. The important process to consider is $B_q^0 - \bar{B}_q^0$ mixing where new effect is expected to occur at tree level. The tree-level transition amplitude is found to be

$$T = \frac{\sqrt{2} G_F}{x} (V_{tq}^* V_{tb})^2 [\bar{q}_L \gamma_\mu b_L] [\bar{q}_L \gamma_\mu b_L]. \quad (54)$$

The new contribution can be compared with the SM prediction which is given by

$$T^{\text{SM}} = \frac{G_F^2 M_W^2}{\pi^2} (V_{tq}^* V_{tb})^2 [\bar{q}_L \gamma_\mu b_L] [\bar{q}_L \gamma_\mu b_L] S(y_t), \quad (55)$$

where $S(y)$ is given in Eq. (50) with $y_t = m_t^2/M_W^2$. After substituting all the relevant variables by their numerical values, we find

$$\frac{\Delta M_{B_q}}{(\Delta M_{B_q})^{\text{SM}}} = \frac{T}{T^{\text{SM}}} = \frac{72}{x}. \quad (56)$$

With the limit on x (> 20) imposed by the Z -pole data alone, we expect the new contribution to reach the level of 360% for the small possible values of x . In the case

that the third and the second generation fermions mix with the maximal strength, the $\text{Br}(\tau \rightarrow \mu \bar{\nu}_\mu \nu_\tau)$ data requires $x > 48$, so that the new contribution to the $B_q^0 - \bar{B}_q^0$ mixing is expected to be less than 150%.

The measured value of $\Delta M_{B_d} = 0.470 \pm 0.019 \text{ ps}^{-1}$ [10] can be turned into an information on the CKM elements product $|V_{td}V_{tb}^*|$ which yields $|V_{td}V_{tb}^*| = 0.0084 \pm 0.0018$ for the SM [10]. In the proposed model, the prediction for ΔM_{B_d} is larger than the SM value by a factor $1 + 72/x$ (adding both SM and the new effect). Therefore, the extracted $|V_{td}V_{tb}^*|$ will be modified accordingly. For example, for $x = 20$, we find $0.0022 < |V_{td}V_{tb}^*| < 0.0056$ at the 2σ level. This shift is not expected to appreciably affect the unitarity condition [18]

$$|V_{td}|^2 + |V_{ts}|^2 + |V_{tb}|^2 = 0.98 \pm 0.30. \quad (57)$$

For example, for $x \geq 20$ the deviation from unity will be of the order $\sim \frac{72}{x}|V_{td}|^2 \lesssim 7 \times 10^{-4}$, which is much smaller than the present errors. Also, it is clear that the predicted ratio $\Delta M_{B_d}/\Delta M_{B_s}$ in our model is the same as the SM prediction. Therefore, the extracted ratio $|V_{td}/V_{ts}|$ yields the same SM result.

Next, we consider the CLEO limit on $\text{Br}(b \rightarrow s \ell^+ \ell^-)$ and study its impact on the model. At tree level, the expected branching ratio is given by

$$\frac{\text{Br}(b \rightarrow s \mu^- \mu^+)}{\text{Br}(b \rightarrow c \mu^- \bar{\nu}_\mu)} = \frac{1}{4x^2} \frac{|V_{ts}V_{tb}|^2}{|V_{cb}|^2 f(z)} \left(\sin^4 \beta - 4 \sin^2 \beta \sin^2 \phi \sin^2 \theta + 8 \sin^4 \theta \sin^4 \phi \right), \quad (58)$$

where $f(z)$ is given in Eq. (37) and where $z = m_c/m_b$ [21, 22]. Using the experimental data $\text{Br}(b \rightarrow c \mu^- \bar{\nu}_\mu) = (10.5 \pm 0.5)\%$ [23], we get

$$\text{Br}(b \rightarrow s \mu^- \mu^+) \lesssim \frac{2.1 \times 10^{-2}}{x^2} \quad (59)$$

after spanning the allowed values of the CKM matrix elements with $\sin^2 \beta = 0.5$ and $\sin^2 \phi = 0.04$. To agree with the CLEO upper limit, which is 5.8×10^{-5} [24], x is found to be larger than 19, which should be compared with the bound ($x > 48$) obtained from the $\text{Br}(\tau \rightarrow \mu \bar{\nu}_\mu \nu_\tau)/\text{Br}(\tau \rightarrow e \bar{\nu}_e \nu_\tau)$ data. To reach the same sensitivity as τ decay for $\sin^2 \beta = 0.5$, the measurement of $\text{Br}(b \rightarrow s \mu^- \mu^+)$ has to be improved by a factor of 10, although in general, they have different dependence on $\sin^2 \beta$.

With the assumption that lepton mixing is only present between the third and the second generation, there is no new contribution to the decay rate of $b \rightarrow s e^+ e^-$. If we assume the opposite, namely that mixing is significant between the first and third generation, then we expect the decay rate of $b \rightarrow s e^+ e^-$ to dominate the decay rate of $b \rightarrow s \mu^+ \mu^-$. Since the CLEO bound on $\text{Br}(b \rightarrow s e^+ e^-)$, less than 5.7×10^{-5} [24], is similar to the bound on the $\mu\mu$ channel, we expect a similar conclusion on constraining the parameter x . Furthermore, the decay rate of $b \rightarrow s e^\pm \mu^\mp$ is highly suppressed because of the sever constraint on the $e\mu$ mixing established from the decay of $\mu \rightarrow eee$ and $\mu \rightarrow e\gamma$, as discussed in section 5. On the other hand, the branching ratio $\text{Br}(b \rightarrow s \mu^\pm \tau^\mp)$ predicted in this model is of the same order as $\text{Br}(b \rightarrow s \mu^- \mu^+)$. In the limit of ignoring the mass difference between τ and μ , it can

be obtained from Eq. (58) by multiplying a factor of $2 \cot^2 \beta$ and setting $\sin^2 \phi = 0$. Since this decay mode is absent in the SM, it can be very useful to further test the model.

Similarly, our model predicts a tree-level contribution to the process $b \rightarrow s\nu\bar{\nu}$, whose branching ratio, when normalized by $\text{Br}(b \rightarrow c\mu^-\bar{\nu}_\mu)$, is given as

$$\frac{\text{Br}(b \rightarrow s\nu\bar{\nu})}{\text{Br}(b \rightarrow c\mu^-\bar{\nu}_\mu)} = \frac{1}{4x^2} \frac{|V_{ts}V_{tb}|^2}{|V_{cb}|^2 f(z)}, \quad (60)$$

where $f(z)$ is given in Eq. (37) and $z = m_c/m_b$ [21, 22]. In the above result we summed over all neutrino flavors, therefore, the $\sin^2 \beta$ dependence cancels. Using the experimental data $\text{Br}(b \rightarrow c\mu^-\bar{\nu}_\mu) = (10.5 \pm 0.5)\%$ [23], we conclude

$$\text{Br}(b \rightarrow s\nu\bar{\nu}) \lesssim \frac{9.1 \times 10^{-2}}{x^2} \quad (61)$$

after spanning the allowed values of the CKM matrix elements. It is interesting to notice that the predicted branching ratio is independent of $\sin^2 \beta$ and $\sin^2 \phi$ similar to the case of $\text{Br}(K^+ \rightarrow \pi^+\nu\bar{\nu})$. To agree with the experimental upper limit, which is 3.9×10^{-4} [25], it requires $x > 15$, independent of the parameters $\sin^2 \phi$ and $\sin^2 \beta$. Currently, for $\text{Br}(b \rightarrow s\nu\bar{\nu})$ to reach the same sensitivity as τ decay for $\sin^2 \beta = 0.5$, the measurement of $\text{Br}(b \rightarrow s\nu\bar{\nu})$ has to be improved by a factor of 10.

Another interesting process to consider is the decay $B_{s,d} \rightarrow \ell^+\ell^-$. At tree level, the decay rate is given by

$$\Gamma(B_q \rightarrow \tau^+\tau^-) = \frac{G_F^2 f_{B_q}^2 m_{B_q} m_\tau^2 |V_{tb}V_{tq}|^2}{4\pi x^2} (\cos^2 \beta - 4 \sin^2 \theta \sin^2 \phi)^2 \left(1 - \frac{4m_\tau^2}{m_{B_q}^2}\right)^{3/2}. \quad (62)$$

Using the values $\cos^2 \beta = 0.5$, $\sin^2 \phi = 0.04$, $m_{B_s} = 5.369$ GeV, and $f_{B_s} = 0.23$ GeV [26], the branching ratio $\text{Br}(B_s \rightarrow \tau^+\tau^-)$ is given as

$$\text{Br}(B_s \rightarrow \tau^+\tau^-) = \frac{4.6 \times 10^{-3}}{x^2}. \quad (63)$$

For $x \geq 48$, it corresponds to $\text{Br}(B_s \rightarrow \tau^+\tau^-) \lesssim 2.0 \times 10^{-6}$, which is of the same order as the SM prediction [21]. For the process $B_d \rightarrow \tau^+\tau^-$, with $m_{B_d} = 5.279$ GeV and $f_{B_d} = 0.18$ GeV [26], the branching ratio $\text{Br}(B_d \rightarrow \tau^+\tau^-)$ is given as

$$\text{Br}(B_d \rightarrow \tau^+\tau^-) = \frac{2.4 \times 10^{-4}}{x^2}. \quad (64)$$

For $x \geq 48$, it corresponds to $\text{Br}(B_d \rightarrow \tau^+\tau^-) \lesssim 1.0 \times 10^{-7}$, which is again of the same order as the SM prediction [21].

Next, consider the decay rates of $B_{s,d} \rightarrow \mu^+\mu^-$. At tree level, the decay rate is given by

$$\Gamma(B_q \rightarrow \mu^+\mu^-) = \frac{G_F^2 f_{B_q}^2 m_{B_q} m_\mu^2 |V_{tb}V_{tq}|^2}{4\pi x^2} (\sin^2 \beta - 4 \sin^2 \theta \sin^2 \phi)^2 \left(1 - \frac{4m_\mu^2}{m_{B_q}^2}\right)^{3/2}. \quad (65)$$

Using the values $\sin^2 \beta = 0.5$, $\sin^2 \phi = 0.04$, and $f_{B_s} = 0.23$ GeV [26], the branching ratio $\text{Br}(B_s \rightarrow \mu^+ \mu^-)$ is given as

$$\text{Br}(B_s \rightarrow \mu^+ \mu^-) = \frac{3.8 \times 10^{-5}}{x^2}. \quad (66)$$

For $x \geq 48$, we find $\text{Br}(B_s \rightarrow \mu^+ \mu^-) \lesssim 1.7 \times 10^{-8}$. This result is smaller than the current experimental upper limit, 2.6×10^{-6} [27], by about two orders of magnitude. Similarly, the branching ratio of $B_d \rightarrow \mu^+ \mu^-$ is given as

$$\text{Br}(B_d \rightarrow \mu^+ \mu^-) = \frac{2.0 \times 10^{-6}}{x^2}. \quad (67)$$

For $x \geq 48$, we find $\text{Br}(B_d \rightarrow \mu^+ \mu^-) \lesssim 8.8 \times 10^{-10}$. Again, this result is smaller than the experimental upper limit, 8.6×10^{-7} [27], by three orders of magnitude.

Finally, we note that in this model, with lepton mixing, it is possible to have the decay modes of $B_{d,s} \rightarrow \mu^\pm \tau^\mp$, which are absent in the SM. In the limit of ignoring the mass difference between τ and μ , with maximal lepton mixing, their branching ratios are about twice of those for the $\tau\tau$ modes. Hence, detecting such non-standard decay modes can further constrain the model, especially on the lepton mixing parameter $\sin^2 \beta$.

In conclusion, under the down-type quark mixing scenario, the decay width of $K^+ \rightarrow \pi^0 e^+ \nu_e$ is not modified at tree level, if assuming the third family lepton does not mix with the first family lepton. The branching ratios of $K^+ \rightarrow \pi^+ \nu \bar{\nu}$ can be an order of magnitude larger than the SM prediction, and can be tested at Kaon factories. The effect to the K^0 - \bar{K}^0 mixing is of the same order as the SM prediction, which can prove to be useful if the long-distance contribution can be better understood theoretically. Similarly, the branching ratio $\text{Br}(b \rightarrow s \nu \bar{\nu})$ is modified and can be an order of magnitude larger than the SM prediction. Furthermore, since the branching ratios $\text{Br}(K^+ \rightarrow \pi^+ \nu \bar{\nu})$ and $\text{Br}(b \rightarrow s \nu \bar{\nu})$ do not depend on $\sin^2 \phi$ and $\sin^2 \beta$, they can be extremely useful in constraining the remaining parameter x .

The current data on the branching ratios of $B_{s,d} \rightarrow \tau^- \tau^+$, $\mu^- \mu^+$ and $b \rightarrow s \mu^- \mu^+$, $s e^- e^+$ does not impose a better constraint on the model than that by the Z -pole measurements. However, with a much larger statistics of the data in the B -factories, we expect it to be improved. Since this model also predicts non-SM decay modes, such as $b \rightarrow s \mu^\pm \tau^\mp$ and $B_{s,d} \rightarrow \mu^\pm \tau^\mp$, with comparable branching ratios, they should be measured to test the model prediction on the lepton mixing dynamics (i.e., $\sin^2 \beta$ dependence). For the range of the parameter x consistent with the Z -pole data, it is found that in this model a new contribution to the B^0 - \bar{B}^0 mixing can reach the range of 150%–360%.

As a summary, in Table 3 we tabulate the predictions of this model for various decay processes. Two cases are considered, one for $\sin^2 \beta = 0.0$ and $x = 20$, another for $\sin^2 \beta = 0.5$ and $x = 48$. For both cases we set $\sin^2 \phi = 0.04$.

6.2 Mixing in the Up-Quark Sector

In this section we assume that no mixing occurs in the down-type quarks, so that $L_d^\dagger G L_d = G$, and $L_u^\dagger G L_u = V G V^\dagger$. In this case, the quark interactions to the gauge bosons are given in Eq. (16) with the above substitutions. Similar to the case of down-type quark mixing, the FCNC interactions are completely determined by the CKM matrix V and the two parameters $\sin^2 \phi$ and x . The matrix $V G V^\dagger$ can be explicitly written as

$$V G V^\dagger = \begin{pmatrix} |V_{ub}|^2 & V_{ub} V_{cb}^* & V_{ub} V_{tb}^* \\ V_{cb} V_{ub}^* & |V_{cb}|^2 & V_{cb} V_{tb}^* \\ V_{tb} V_{ub}^* & V_{tb} V_{cb}^* & |V_{tb}|^2 \end{pmatrix}. \quad (68)$$

Again, because the elements of the matrix $V^\dagger G V$ are naturally small, we do not expect large effects in the FCNC processes.

6.2.1 Charged-Current Phenomenology

The non-standard contribution to charged-current processes is given by Eq. (46). In terms of the mass eigenstates and assuming no mixing in the down-type quarks, j_h^- contains the following charged currents:

$$j_h^- = V_{ub} \overline{u}_L \gamma_\mu b_L, \quad V_{cb} \overline{c}_L \gamma_\mu b_L, \quad V_{tb} \overline{t}_L \gamma_\mu b_L. \quad (69)$$

It is important to note that only the b quark, among the down-type quarks, appears in j_h^- , which implies that new effects in the charged currents must involve the b quark. Because the non-standard contribution has the form $j_h^+ j_h^-$, the only non-vanishing effect we expect in the pure hadronic charged-current interaction (at the leading order in $1/x$) is that with a b quark in both currents, i.e., with $\Delta B = 0$. Therefore, no new effect is expected in any of the hadronic decay channel of K , D , and B mesons.

Next, let us consider the semi-leptonic decay processes. The relevant hadronic currents are

$$V_{ub} \overline{u}_L \gamma_\mu b_L, \quad V_{cb} \overline{c}_L \gamma_\mu b_L, \quad (70)$$

while the relevant leptonic currents are

$$\sin^2 \beta \overline{\mu}_L \gamma_\mu \nu_{\mu L}, \quad \cos^2 \beta \overline{\tau}_L \gamma_\mu \nu_{\tau L}, \quad \sin \beta \cos \beta \overline{\mu}_L \gamma_\mu \nu_{\tau L}, \quad \sin \beta \cos \beta \overline{\tau}_L \gamma_\mu \nu_{\mu L}. \quad (71)$$

It is clear that new effects in the charged-current semi-leptonic decays are only expected in the b -quark system. Explicitly, the decay processes $b \rightarrow u (\mu, \tau)(\nu_\mu, \nu_\tau)$ will receive new contributions induced by the following interaction terms:

$$\begin{aligned} & \frac{2\sqrt{2}G_F V_{ub}}{x} \left\{ \sin^2 \beta (\overline{u}_L \gamma_\mu b_L) (\overline{\mu}_L \gamma_\mu \nu_{\mu L}), \quad \cos^2 \beta (\overline{u}_L \gamma_\mu b_L) (\overline{\tau}_L \gamma_\mu \nu_{\tau L}) \right\}, \\ & \frac{2\sqrt{2}G_F V_{ub} \sin \beta \cos \beta}{x} \left\{ (\overline{u}_L \gamma_\mu b_L) (\overline{\mu}_L \gamma_\mu \nu_{\tau L}), \quad (\overline{u}_L \gamma_\mu b_L) (\overline{\tau}_L \gamma_\mu \nu_{\mu L}) \right\}. \end{aligned}$$

A similar expression for the b decay to charm can be obtained with V_{ub} replaced by V_{cb} . Hence, we expect an increase in the b -quark semi-leptonic decays as compared to the SM. As an example, the branching ratio of $B_d^0 \rightarrow D^- \ell^+ \nu$ and $B_s^0 \rightarrow D_s^- \ell^+ \nu$ is predicted to be

$$\text{Br}(B^0 \rightarrow D^- \ell^+ \nu) = \text{Br}^{\text{SM}}(B^0 \rightarrow D^- \ell^+ \nu) \left(1 + \frac{2}{x}\right), \quad (72)$$

where all the three lepton (including neutrino) flavors are included. (Note that the $\sin^2 \beta$ dependence cancels.) With $x > 20$, imposed by Z -pole data, we do not expect the new physics effect to exceed 10%. Because of the large uncertainty (exceeding 25% [10]) of present data, these processes do not offer a stringent constraint on the model. With more statistics of the future data, these decay processes can be useful for constraining the parameter x .

Under this scenario, we conclude that the values of the CKM matrix elements extracted from tree-level processes not involving the b quark are not modified by the model. In other words, the extracted values of the CKM elements, V_{ud} , V_{us} , V_{cd} , and V_{cs} , for the SM and this model coincide. However, the matrix elements V_{ub} and V_{cb} are modified slightly. To explore this effect, let us consider the transition $b \rightarrow u \mu^- \bar{\nu}_\mu$. Its amplitude is modified with V_{ub} replaced by $V_{ub}(1 + \sin^2 \beta/x)$. Therefore, the extracted experimental value of V_{ub} , assuming the validity of the SM, is equivalent to the quantity $V_{ub}(1 + \sin^2 \beta/x)$ in this model. From the data, the unitarity condition for the SM reads as [18]

$$|V_{ud}|^2 + |V_{us}|^2 + |V_{ub}|^2 = 0.997 \pm 0.002. \quad (73)$$

Hence, at the 2σ level, we conclude that $x \geq 0.05 \sin^2 \beta$. It is clear that the unitarity condition does not add any useful constraint on the model after testing against the Z -pole data which requires $x > 20$.

6.2.2 Neutral-Current Phenomenology

First, let us consider neutral-current processes of hadron-hadron interactions. In this case, the relevant neutral currents are

$$j_h^3 = \bar{t}_L \gamma_\mu \left(\frac{1}{2}\right) t_L, \bar{b}_L \gamma_\mu \left(-\frac{1}{2}\right) b_L, \quad (74)$$

written in terms of the weak eigenstates, which yields the following four-fermion interaction current in terms of the mass eigenstates:

$$|V_{ub}|^2 \bar{u}_L \gamma_\mu u_L, |V_{cb}|^2 \bar{c}_L \gamma_\mu c_L, V_{ub} V_{cb}^* \bar{u}_L \gamma_\mu c_L. \quad (75)$$

In the four-fermion neutral-current interaction we notice that the d and s quarks will appear only through the electromagnetic current J_{em} (cf. Eq. (23)). Because of the structure of the neutral-current interaction, new physics can only contribute to processes with $\Delta B = 0$. Thus, neither the B hadronic decay nor the B^0 - \bar{B}^0 mixing

is modified at tree level in this model. Similarly, we conclude that new effects must have $\Delta S = 0$ in pure hadronic interaction. Therefore, K^0 - \overline{K}^0 mixing is not modified. We conclude that new physics effects, in the pure hadronic decay modes, are only expected in the c -quark decay channels. Nevertheless, these new physics effects are naturally small because the FCNC couplings predicted by this model at tree level are suppressed by products of CKM matrix elements.

Second, let us consider the semi-leptonic decays. Again, we do not expect any new effects in the b -quark semi-leptonic decays because of the requirement $\Delta B = 0$. Effects are only expected in the charm decay where we get interactions of the form

$$\frac{\sqrt{2}G_F}{x} V_{ub}^* V_{cb} (\overline{u}_L \gamma^\mu c_L) \left(\sin^2 \beta (\overline{\mu}_L \gamma_\mu \mu_L) - 2 \sin^2 \phi \sin^2 \theta (\overline{\mu} \gamma_\mu \mu) \right). \quad (76)$$

Because of the large suppression factor $V_{ub}^* V_{cb}$ and large error on present experimental data, it is extremely difficult to gain any further information about the model from the semi-leptonic decay channels of charm hadrons.

The only suspected new effect in the b -quark system is through the $\Upsilon(1S)$ decay. In this case, the decay proceeds through $b\overline{b} \rightarrow \gamma, Z, Z' \rightarrow \mu^+ \mu^-$. At tree level, the new contribution is expressed through the interaction term

$$\frac{\sqrt{2}G_F}{x} \left((\overline{b}_L \gamma^\mu b_L) - \frac{2}{3} \sin^2 \phi \sin^2 \theta (\overline{b} \gamma_\mu b) \right) \left(\sin^2 \beta (\overline{\mu}_L \gamma_\mu \mu_L) - 2 \sin^2 \phi \sin^2 \theta (\overline{\mu} \gamma_\mu \mu) \right). \quad (77)$$

For very small values of $\sin^2 \phi$ and for large possible lepton mixing (i.e., large $\sin^2 \beta$), we can approximate the above interaction relevant to $\Upsilon(1S) \rightarrow \mu^+ \mu^-$ as

$$\frac{\sqrt{2}G_F \sin^2 \beta}{x} (\overline{b}_L \gamma^\mu b_L) (\overline{\mu}_L \gamma_\mu \mu_L). \quad (78)$$

Needless to say, the dominant contribution to the $\Upsilon(1S)$ decay width is coming from the photon exchange. The non-standard contribution predicted by this model can be estimated as follows. The amplitude $\Upsilon(1S) \rightarrow \ell^+ \ell^-$ can in general be written as [2]

$$T(\Upsilon(1S) \rightarrow \ell^+ \ell^-) = -\frac{4\pi\alpha}{3M_\Upsilon^2} \langle 0 | (b\overline{b})_V | \Upsilon \rangle [r_V(\ell\ell)_V + r_A(\ell\ell)_A]. \quad (79)$$

For the dominant photon contribution, $r_V = 1$ and $r_A = 0$. In the case of τ lepton mode, these couplings in the proposed model will be modified into

$$r_V = 1 - \frac{3M_\Upsilon^2 \cos^2 \beta}{16 \sin^2 \theta M_W^2 x}, \quad (80)$$

$$r_A = \frac{3M_\Upsilon^2 \cos^2 \beta}{16 \sin^2 \theta M_W^2 x}. \quad (81)$$

A similar relation holds for the μ lepton mode, but with $\cos^2 \beta$ replaced by $\sin^2 \beta$. The ratio of the τ lepton decay rate to the μ lepton decay rate is

$$\frac{\Gamma(\Upsilon(1S) \rightarrow \tau^+ \tau^-)}{\Gamma(\Upsilon(1S) \rightarrow \mu^+ \mu^-)} = \sqrt{1 - 4 \frac{m_\tau^2}{M_\Upsilon^2}} \left(1 + 2 \frac{m_\tau^2}{M_\Upsilon^2} \right) \left[1 - \frac{3M_\Upsilon^2}{8 \sin^2 \theta M_W^2 x} (\cos^2 \beta - \sin^2 \beta) \right], \quad (82)$$

which amounts to new effect of the order

$$- 2.3 \times 10^{-2} \frac{1}{x} (\cos^2 \beta - \sin^2 \beta) . \quad (83)$$

Therefore, the expected maximal deviation is less than $\pm 0.1\%$, for $x \geq 20$. (It vanishes for the maximal lepton mixing scenario, i.e. for $\sin^2 \beta = 0.5$.) The current experimental error is at the percent level [10], so that it does not provide additional constraints on the model. However, it is interesting to notice that the sign of the deviation is governed by the difference $\cos^2 \beta - \sin^2 \beta$. Future measurements with a much less error can be used to determine the lepton mixing angle. Finally, we note that the non-SM decay mode $\Upsilon(1S) \rightarrow \mu^\pm \tau^\mp$ is expected by this model with a branching ratio less than 4×10^{-10} . Since this decay process is not allowed by the SM, it can provide a significant constraint on the lepton mixing parameter $\sin^2 \beta$.

The above discussion is valid for tree-level contributions. We now consider whether one-loop effects can be significant to some observables, such as the K^0 - \overline{K}^0 , B^0 - \overline{B}^0 mixing, and the decay branching ratio of $b \rightarrow s\gamma$.

6.2.3 One-Loop Effects

In the SM, K^0 - \overline{K}^0 and B^0 - \overline{B}^0 mixing are induced via one-loop W - W exchange box diagrams. In this model and under the scenario of a trivial L_d , the K^0 - \overline{K}^0 and B^0 - \overline{B}^0 mixing can occur at the one-loop level through box diagrams involving the exchange of W and/or W' gauge bosons. In addition to the SM diagrams, there are four box diagrams with one W and one W' exchange. Diagrams with two W' exchange do not contribute at the order $1/x$ but at the higher order $1/x^2$.

For the case of K^0 - \overline{K}^0 mixing, we calculate the one-loop amplitude and compare with the short distance contribution of the SM. Substituting the values of M_W , m_t , m_c , and the V_{CKM} elements [10], we find

$$\frac{T}{T^{\text{SM}}} = \frac{\Delta M}{\Delta M^{\text{SM}}} \lesssim 3.4 \times 10^{-3} \frac{\sin^4 \phi}{x} . \quad (84)$$

Since constraints imposed by the Z -pole data require $\sin^2 \phi/x < 0.3\%$, new effect to the K^0 - \overline{K}^0 are extremely small and of no relevance to the discussion.

Next, let us consider the B_q - \overline{B}_q mixing. The leading SM one loop amplitude is given in Eq. (55). Similar to the K^0 - \overline{K}^0 case, we include the additional box diagrams that contribute at the order $1/x$, we find

$$\frac{T}{T^{\text{SM}}} = \frac{\Delta M_q}{\Delta M_q^{\text{SM}}} = \frac{2 \sin^2 \phi}{x} - 2.24 \frac{\sin^4 \phi}{x} . \quad (85)$$

Using the Z -pole constraint ($x > 20$ for $\sin^2 \phi > 0.04$), we expect new effect to the amplitude not to exceed 0.4% relative to the SM. Therefore, we do not expect large new effect to the B_q - \overline{B}_q mixing at the one-loop level for the case of trivial L_d .

Finally, let us consider the decay of $b \rightarrow s\gamma$. The SM amplitude for the process $b \rightarrow s\gamma$ is given by [28]

$$T^{\text{SM}} = \frac{1}{16\pi^2} \frac{m_b}{M^2} \left(\frac{eg^2}{4} V_{ts}^* V_{tb} \right) [\bar{u}_s (1 + \gamma_5) (2p \cdot \varepsilon - \varepsilon_\mu \gamma^\mu) u_b] \{T_1 + T_2\}, \quad (86)$$

where

$$T_1 = \frac{1}{(y-1)^4} \left[\frac{y^4}{2} + \frac{3}{4}y^3 - \frac{3}{2}y^2 + \frac{1}{4}y - \frac{3}{2}y^3 \ln y \right], \quad (87)$$

$$T_2 = \frac{Q_t}{(y-1)^4} \left[\frac{y^4}{4} - \frac{3}{2}y^3 + \frac{3}{4}y^2 + \frac{1}{2}y + \frac{3}{2}y^2 \ln y \right], \quad (88)$$

and $Q_t = 2/3$ is the electric charge of the top quark.

In this model, the $b \rightarrow s\gamma$ amplitude will be slightly changed due to the modified couplings. The only diagrams we need to consider are the usual W exchange penguin diagrams. Since the fermion couplings are slightly modified, these diagrams will contain an extra contribution with respect to the SM. The penguin diagrams with W' exchange do not contribute to the order $1/x$. We calculate the new amplitude as predicted by the model and compare it to the SM one. After substituting the values of M_W and m_t , we find

$$\frac{T}{T^{\text{SM}}} = -1.7 \frac{\sin^2 \phi}{x} + 1.4 \frac{\sin^4 \phi}{x}. \quad (89)$$

Therefore, for the Z -pole limit ($x > 20$), we expect new contribution not to exceed 0.3% of the SM.

In conclusion, under the up-type quark mixing scenario, this model does not modify the $K^0\text{-}\bar{K}^0$, $B^0\text{-}\bar{B}^0$ mixing, and the decay width of $b \rightarrow s\gamma$ at tree level. The one-loop effects to these observables are small, and do not exceed the level of 0.4% of the SM values. In general, we conclude that the up-type quarks mixing scenario can hardly be examined against the low-energy data available so far.

6.3 The general mixing scenario

In this section, we consider the general case of both types of quark mixing, i.e, where both L_u and L_d are non-trivial. The charged-current mixing matrix V is defined the same as before, $V = L_u^\dagger L_d$. The interaction Lagrangian can be expressed using two matrix structures, such as V and $L_d^\dagger G L_d$. In this case $L_u^\dagger G L_u = V L_d^\dagger G L_d V^\dagger$. Therefore, under the general mixing scenario, there are additional free parameters in comparison with the previously discussed two cases. The additional parameters appear in the matrix $L_d^\dagger G L_d$, where

$$L_d^\dagger G L_d = \begin{pmatrix} |d_{31}|^2 & d_{31}^* d_{32} & d_{31}^* d_{33} \\ d_{31} d_{32}^* & |d_{32}|^2 & d_{32}^* d_{33} \\ d_{31} d_{33}^* & d_{32} d_{33}^* & |d_{33}|^2 \end{pmatrix}. \quad (90)$$

Since unitarity condition implies that $|d_{31}|^2 + |d_{32}|^2 + |d_{33}|^2 = 1$, there are only two additional free parameters which will be assumed to be real numbers hereafter. (Additional phases can be generated which would signal a new source of CP violation.)

The general case is more tolerant to accommodate low-energy data because of the additional parameters. Nevertheless, as to be shown later, we can set significant constraints on some combination of those additional parameters. In the following, we shall examine a few relevant tree-level FCNC processes.

As a start, we consider the decay $K^+ \rightarrow \pi^+ \nu \bar{\nu}$. As discussed before, this process can occur in this model at tree level through the flavor-changing neutral current $s \rightarrow d Z \rightarrow d \nu \bar{\nu}$. The branching ratio of this process can be obtained from the ratio

$$R = \frac{\text{Br}(K^+ \rightarrow \pi^+ \nu \bar{\nu})}{\text{Br}(K^+ \rightarrow \pi^0 e^+ \nu_e)} = \frac{1}{4x^2} \left(\frac{|d_{31}|^2 |d_{32}|^2}{|V_{us}|^2} \right), \quad (91)$$

which noticeably is independent of the parameters $\sin^2 \beta$ and $\sin^2 \phi$. Therefore, the ratio R can be used to directly set a limit on $|d_{31} d_{32}|/x$, without any assumptions regarding other parameters. If we compare this result with the published result of the E787 collaboration [20], $\text{Br}(K^+ \rightarrow \pi^+ \nu \bar{\nu}) = 4.2_{-3.5}^{+9.7} \times 10^{-10}$, we obtain the 2σ level constraint:

$$\frac{|d_{31} d_{32}|}{x} \lesssim 10^{-4}. \quad (92)$$

For $x = 20$, the smallest value of x consistent with the Z -pole data, it requires $|d_{31} d_{32}| < 2 \times 10^{-3}$.

Now we consider the new effect to the K^0 - \bar{K}^0 mixing. A straightforward calculation of the tree-level amplitude as compared with the SM short distance contribution gives

$$\frac{T}{T^{\text{SM}}} = \frac{\Delta M}{\Delta M^{\text{SM}}} \approx 1 \times 10^7 \frac{\text{Re}(d_{31}^* d_{32})^2}{x}. \quad (93)$$

Combined with the previous constraint derived from $K^+ \rightarrow \pi^+ \nu \bar{\nu}$, we conclude

$$\frac{\Delta M}{\Delta M^{\text{SM}}} \lesssim 1 \times 10^3 |d_{31} d_{32}|. \quad (94)$$

Hence, the combination of the $K^+ \rightarrow \pi^+ \nu \bar{\nu}$ and K^0 - \bar{K}^0 mixing data directly constrains the magnitude of $|d_{31} d_{32}|$ because the explicit x dependence cancels. If $x = 20$, the non-standard contribution in K^0 - \bar{K}^0 mixing can be as large as twice the SM short distance contribution.

Next, we use bottom physics data to constrain the second additional free parameter. Consider the decay rate $b \rightarrow s \nu \bar{\nu}$. The expected branching ratio, which is independent of the parameters $\sin^2 \phi$ and $\sin^2 \beta$, is given by

$$\frac{\text{Br}(b \rightarrow s \nu \bar{\nu})}{\text{Br}(b \rightarrow c \mu^- \bar{\nu}_\mu)} = \frac{1}{4x^2} \frac{|d_{32} d_{33}|^2}{|V_{cb}|^2 f(z)}, \quad (95)$$

where $f(z)$ is given in Eq. (37) and $z = m_c/m_b$. Using the experimental data, $\text{Br}(b \rightarrow c \mu^- \bar{\nu}_\mu) = (10.5 \pm 0.5)\%$ [23] and $\text{Br}(b \rightarrow s \nu \bar{\nu}) < 3.9 \times 10^{-4}$ [25], we obtain

the constraint

$$\frac{|d_{32}d_{33}|}{x} < 2.9 \times 10^{-3}, \quad (96)$$

For $x = 20$, it requires $|d_{32}d_{33}| < 0.06$. Next, we consider the B_s^0 - \overline{B}_s^0 mixing. A straightforward calculation of the new physics effect to the B_s^0 - \overline{B}_s^0 mixing compared with the SM contribution gives

$$\frac{T}{T^{\text{SM}}} = \frac{\Delta M_{B_s}}{(\Delta M_{B_s})^{\text{SM}}} \approx 3.4 \times 10^4 \frac{\text{Re}(d_{32}^* d_{33})^2}{x}. \quad (97)$$

When combined with the previous constraint derived from the measurement of $\text{Br}(b \rightarrow s\nu\overline{\nu})$, it yields

$$\frac{\Delta M_{B_s}}{(\Delta M_{B_s})^{\text{SM}}} \lesssim 100 |d_{32}d_{33}|. \quad (98)$$

Hence, the combination of the $b \rightarrow s\nu\overline{\nu}$ and B_s^0 - \overline{B}_s^0 mixing data directly constrains the magnitude of $|d_{32}d_{33}|$ because the explicit x dependence cancels. For $x = 20$, the non-standard contribution to B_s^0 - \overline{B}_s^0 mixing can be as large as six times the SM short distance contribution.

Given the constraints on $|d_{31}d_{32}|$, $|d_{32}d_{33}|$, and the unitarity condition on the matrix L_d , one can derive the allowed space of the parameters $|d_{31}|$, $|d_{32}|$, and $|d_{33}|$. It is interesting to notice that in the SM neither L_u nor L_d can be separately determined, and only the CKM matrix V , which is the product of L_u^\dagger and L_d , can be measured experimentally. However, in this model, the elements in the third column of the $L_{u,d}$ mixing matrices can be determined, and can be further constrained by including other low-energy data. Unfortunately, in general, those observables depend also on some other parameters, such as $\sin^2 \phi$ and $\sin^2 \beta$, of the model. Some of them are discussed below.

The expected branching ratio for $b \rightarrow s\mu^+\mu^-$ is given by

$$\frac{\text{Br}(b \rightarrow s\mu^-\mu^+)}{\text{Br}(b \rightarrow c\mu^-\overline{\nu}_\mu)} = \frac{1}{4x^2} \frac{|d_{32}|^2 |d_{33}|^2}{|V_{cb}|^2 f(z)} \left(\sin^4 \beta - 4 \sin^2 \beta \sin^2 \phi \sin^2 \theta + 8 \sin^4 \theta \sin^4 \phi \right). \quad (99)$$

Using the CLEO data [23], we obtain

$$\frac{|d_{32}d_{33}|}{x} < 2.4 \times 10^{-3}, \quad (100)$$

for $\sin^2 \beta = 0.5$ and $\sin^2 \phi = 0.04$. For $x = 48$, the minimal value of x consistent with Z-pole data and τ life-time, it requires $|d_{32}d_{33}| < 0.12$.

Next, consider the decay rate of $B_{s,d} \rightarrow \mu^+\mu^-$. The tree level contribution gives

$$\Gamma(B_s \rightarrow \mu^+\mu^-) = \frac{G_F^2 f_{B_q}^2 m_{B_q} m_\mu^2 |d_{32}d_{33}|^2}{4\pi x^2} \left(\sin^2 \beta - 4 \sin^2 \theta \sin^2 \phi \right)^2 \left(1 - \frac{4m_\mu^2}{m_{B_q}^2} \right)^{3/2}. \quad (101)$$

For $\sin^2 \beta = 0.5$ and $\sin^2 \phi = 0.04$, the branching ratio $\text{Br}(B_s \rightarrow \mu^+ \mu^-)$ is

$$\text{Br}(B_s \rightarrow \mu^+ \mu^-) = 0.018 \frac{|d_{32} d_{33}|^2}{x^2}. \quad (102)$$

Comparing this result with the experimental upper limit [27], we obtain

$$\frac{|d_{32} d_{33}|}{x} < 1.2 \times 10^{-2}. \quad (103)$$

This constraint is not as strong as the one obtained from $b \rightarrow s \mu^+ \mu^-$, the latter is stronger by one order of magnitude.

The branching ratio of $B_d \rightarrow \mu^+ \mu^-$, for $\sin^2 \beta = 0.5$ and $\sin^2 \phi = 0.04$, is

$$\text{Br}(B_d \rightarrow \mu^+ \mu^-) = 0.01 \frac{|d_{31} d_{33}|^2}{x^2}. \quad (104)$$

Comparing this result with the experimental upper limit [27], we obtain

$$\frac{|d_{31} d_{33}|}{x} < 9.1 \times 10^{-3}. \quad (105)$$

For $x = 48$, it yields $|d_{31} d_{33}| < 0.44$.

The new physics effect to the $B_d^0 - \overline{B}_d^0$ mixing compared with the SM contribution can be written as

$$\frac{\Delta M_{B_d}}{(\Delta M_{B_d})^{\text{SM}}} = \frac{T}{T^{\text{SM}}} \approx 3.6 \times 10^5 \frac{\text{Re}(d_{31}^* d_{33})^2}{x}. \quad (106)$$

When combined with the above constraint derived from the decay $B_d \rightarrow \mu^+ \mu^-$ [27], it yields

$$\frac{\Delta M_{B_d}}{(\Delta M_{B_d})^{\text{SM}}} \lesssim 3.3 \times 10^3 |d_{31} d_{33}|. \quad (107)$$

If we consider the values $x = 48$, $\sin^2 \beta = 0.5$, and $\sin^2 \phi = 0.04$, then $|d_{31} d_{33}| < 0.44$ and $\Delta M_{B_d}/(\Delta M_{B_d})^{\text{SM}} \lesssim 1450$, which implies that the current measurement of $\text{Br}(B_d \rightarrow \mu^+ \mu^-)$ is not useful to constrain this model, and new physics effect to $B_d^0 - \overline{B}_d^0$ mixing can be much larger than the SM prediction. A precision measurement of $B_d^0 - \overline{B}_d^0$ mixing will be extremely valuable to test this model with the scenario that both the up- and down-type quarks can mix in their mass eigenstates.

Similar to the discussions given for the other two scenarios, this model also allows lepton number violation processes, such as $B_{s,d} \rightarrow \mu^\pm \tau^\mp$ and $b \rightarrow s \mu^\pm \tau^\mp$. Since their branching ratios are of the same order as those for the $\tau^+ \tau^-$ mode, they can be very useful for further testing the model. In conclusion, under the general mixing scenario, the model requires two additional free (real) parameters, although additional phases can be introduced to generate a new source of CP violation. Depending on the values of the parameters, sizable effects in various FCNC processes are expected. In Table 4, we summarize the results of this section by giving the constraints on the mixing parameters as extracted from different experiments.

7 Conclusions

In this work, we revisit the model in Ref. [5], and update the constraints on this model from the Z -pole data at LEP/SLC. We find that the heavy gauge boson mass is bounded from below to be about 1.7 TeV at the 2σ level. The parameter x , the square of the ratio of the two VEVs involved in the breaking pattern of the gauge symmetry, is larger than 20 assuming no lepton mixing, and 48 with the maximal possible lepton mixing between μ and τ . Given that, we study the potential of the new physics effect predicted by this model to low-energy data with zero momentum transfer, such as K and B physics. We concentrate on the region where x is large. Using an effective current-current interaction Lagrangian, we systematically examine the possible new physics effects in the charged-current and the neutral-current interactions. We show that FCNC couplings in this model can be written as the product of CKM matrix elements, so that FCNC processes are naturally suppressed. To examine how well low-energy data can further test this model, we have separately studied three different scenarios of quark mixing.

Assuming the third family lepton does not mix with the first family lepton, the partial decay width of $\mu \rightarrow eee$ and $\mu \rightarrow e\gamma$ will not be modified. The current data on the measurement of the ratio $\Gamma(\tau \rightarrow \mu\bar{\nu}_\mu\nu_\tau)/\Gamma(\tau \rightarrow e\bar{\nu}_e\nu_\tau)$ places the strongest constraint on the parameter x , which is even better than Z -pole constraint for $\sin^2\phi < 0.1$ (cf. Figure 2). The lepton number violation process $\tau \rightarrow \mu\mu\mu$ is also significant and gives a compatible constraint as the above measurement. On the other hand, given the current experimental data, the decay process $\tau \rightarrow \mu\gamma$ and the measurement of the anomalous magnetic dipole moment of the muon are not yet significant in constraining the model. If the above discussed processes can be measured to a better accuracy in future experiments, they will play a more significant role in testing the model considered in this work.

Under the down-type quark mixing scenario, the decay width of $K^+ \rightarrow \pi^0 e^+ \nu_e$ is not modified at tree level, if assuming the third family lepton does not mix with the first family lepton. The branching ratio of $K^+ \rightarrow \pi^+ \nu \bar{\nu}$ can be an order of magnitude larger than the SM prediction. In that case, it can be tested at Kaon factories. The effect to the K^0 - \bar{K}^0 mixing is of the same order as the SM prediction, which can only be useful if the long distance contribution can be better understood theoretically. Furthermore, since the above observables do not depend on the parameter $\sin^2\phi$, they can directly constrain the parameter x of the model. The current data on the branching ratios of $B_{s,d} \rightarrow \tau^- \tau^+, \mu^- \mu^+$ and $b \rightarrow s\mu^- \mu^+, se^- e^+, s\nu \bar{\nu}$ do not impose a better constraint on the model than that by the Z -pole measurements. However, with a much larger statistics of the data in B (Beauty) factories, we expect it to be improved. Since this model also predicts the non-SM decay modes, such as $b \rightarrow s\mu^\pm \tau^\mp$ and $B_{s,d} \rightarrow \mu^\pm \tau^\mp$, with comparable branching ratios, they should be measured to test the model prediction on the lepton mixing dynamics (i.e., $\sin^2\beta$ dependence). For the range of the parameter x consistent with the Z -pole data, it is found that in this model a new contribution to the B_q^0 - \bar{B}_q^0 mixing can reach the range of 150%–360%. Hence, this measurement is useful for testing the model. As a summary to

this scenario, in Table 2 we give the lower bound on the parameter x derived from including the low energy data as well as the Z -pole data. We consider two cases. Case I: No lepton mixing ($\sin^2 \beta = 0$). Case II: Maximal lepton mixing ($\sin^2 \beta = 0.5$). In both cases we set $\sin^2 \phi = 0.04$, since it corresponds to the minimal value of x . Also, in Table 3 we tabulate the predictions of our model for various processes and for two cases. Case I: No lepton mixing ($\sin^2 \beta = 0.0$) and $x = 20$. Case II: Maximal lepton mixing ($\sin^2 \beta = 0.5$) and $x = 48$. For both cases we set $\sin^2 \phi = 0.04$.

Under the scenario of up-type quark mixing, there will be no non-standard effect present in the hadronic decays of K , D and B mesons. This is because in the pure hadronic charged-current interaction, the new physics effect is only expected in processes that involve the b quark and where ΔB vanishes. Furthermore, the present data of semi-leptonic b -quark decays is not accurate enough to further constrain the model, though it can be improved in the B factories. Under this scenario, the unitarity condition of the CKM matrix is modified, but its change is extremely small for the values of x that agree with Z -pole data. In this case, this model does not modify either the B^0 - \overline{B}^0 or the K^0 - \overline{K}^0 mixing at tree level. Although FCNC decay of charm meson is expected to be modified, the non-standard effect is very small because of the natural suppression imposed by the tree level FCNC couplings (which are the product of CKM matrix elements). With enough data in future experiments, the measurement of the partial decay widths of $\Upsilon(1S)$ into the $\tau^+\tau^-$, $\mu^+\mu^-$, and $\mu^\pm\tau^\mp$ modes can further test the model. Furthermore, it can also modify the K^0 - \overline{K}^0 , B^0 - \overline{B}^0 mixing and the decay width of $b \rightarrow s\gamma$ at one-loop level. However, the one-loop effects are small compared to the SM predictions and do not exceed the level of 0.4% of the SM values.

Under the general mixing scenario, the model requires two additional free (real) parameters, although additional phases can be introduced to generate a new source of CP violation. Depending on the values of the parameters, sizable effects in various FCNC processes are expected. Therefore, low-energy data can also test the model with a general mixing scenario. In Table 4 we summarize the results of the general mixing scenario by giving the constraints on the mixing parameters as extracted from different experiments. The general mixing scenario also allows lepton number violation processes, such as $B_{s,d} \rightarrow \mu^\pm\tau^\mp$ and $b \rightarrow s\mu^\pm\tau^\mp$. Since their branching ratios are of the same order as those for the $\tau^+\tau^-$ mode, they can be very useful for further testing the model.

It is interesting to notice that in the SM neither L_u nor L_d can be separately determined, and only the CKM matrix V , which is the product of L_u^\dagger and L_d , can be measured experimentally. However, in this model, the elements in the third column of the $L_{u,d}$ mixing matrices can be determined, and can be further constrained by including other low-energy data. Unfortunately, in general, those observables also depend on some other parameters, such as $\sin^2 \phi$ and $\sin^2 \beta$, of the model.

8 Acknowledgments

E.M. would like to thank K. Hagiwara, Y. Okada, for useful discussion and comments. He also thanks KEK for the kind hospitality, where part of this work was done, and the Matsumae International Foundation for their Fellowship to support his visit in Japan. This work was supported in part by the U.S. NSF under grant PHY-9802564.

References

- [1] C. T. Hill, Phys. Lett. **B266**, 419 (1991); Phys. Lett. **B345**, 483 (1995); S.P. Martin, Phys. Rev. **D46**, 2197 (1992); Phys. Rev. **D45**, 4283 (1992); Nucl. Phys. **B398**, 359 (1993); M. Lindner and D. Ross, Nucl. Phys. **B370**, 30 (1992); R. Bonisch, Phys. Lett. **B268**, 394 (1991); C.T. Hill, D. Kennedy, T. Onogi, and H.L. Yu, Phys. Rev. **D47**, 2940 (1993).
- [2] G. Buchalla, G. Burdman, C.T. Hill, and D. Kominis, Phys. Rev. **D53**, 5185 (1996).
- [3] R.S. Chivukula, E.H. Simmons, J. Terning, Phys. Lett. **B331**, 383 (1994); *ibid*, Phys. Rev. **D53**, 5258 (1996).
- [4] X. Li and E. Ma, Phys. Rev. Lett. **47**, 1788 (1981); E. Ma, X. Li, and S.F. Tuan Phys. Rev. Lett. **60**, 495 (1988); X. Li and E. Ma, Phys. Rev. **D46**, 1905 (1992); J. Phys. **G19**, 1265 (1993).
- [5] E. Malkawi, T. Tait, and C.-P. Yuan. Phys. Lett. **B385**, 304 (1996).
- [6] D.J. Muller and S. Nandi, Phys. Lett. **B383**, 345 (1996).
- [7] J.C. Lee and K.Y. Lee, Phys. Rev. **D58**, 115001 (1998); J.C. Lee and K.Y. Lee, and J.K. Kim, Phys. Lett. **B424**, 133 (1998).
- [8] A. Donini, F. Feruglio, J. Matias, F. Zwirner, Nucl. Phys. **B507**, 51 (1997).
- [9] The LEP Electroweak Working group and the SLD Heavy Flavor Group, CERN-PPE/97-154, December 1997.
- [10] Review of Particle Properties, *The European Physical Journal* **C3**, 1 (1998), and the www page, <http://pdg.lbl.gov>.
- [11] K. Hagiwara, Annu. Rev. Nucl. Part. Sci. **48**, 463 (1998).
- [12] H. Georgi, E.E. Jenkins, and E.H. Simmons, Phys. Rev. Lett **62**, 2789 (1989); *ibid.*, Nucl. Phys. **B331**, 541 (1990); R.S. Chivukula, E.H. Simmons and J. Terning, Phys.Lett. **B346**, 284 (1995).
- [13] I. Park, Nucl. Phys. Proc. Supp. **65**, 136 (1998); M. Schmidtler, Nucl. Phys. Proc. Supp. **65**, 142 (1998).
- [14] B.L. Roberts et al, The E821 Collaboration. Published in the proceedings of the 28th International Conference on High-Energy Physics (ICHEP 96), Warsaw, Poland. World Scientific, River Edge, NJ, 1997, pp. 1035. R.M. Carey, Phys. Rev. Lett. **82**, 1632 (1999).
- [15] Andrzej Czarnecki and Bernd Krause, Nucl. Phys. Proc. Suppl. **51C**, 148 (1996); and the references therein.

- [16] V. Antonelli, S. Bertolini, M. Fabbrichesi, and E.I. Lashin, Nucl. Phys. **B493**, 281 (1997).
- [17] T. Inami and C.S. Lim, Prog. Theor. Phys. **65**, 297 (1981).
- [18] A. Ali and B. Kayser, hep-ph/9806230.
- [19] J. Ellis and J.S. Hagelin, Nucl. Phys. **B217**, 189 (1983); D. Rein and L.M. Sehgal, Phys. Rev. **D39**, 3325 (1989); J.S. Hagelin and L.S. Littenberg, Prog. Part. Nucl. Phys. **23**, 1 (1989); C.Q. Gang, I.J. Hsu, and Y.C. Lin, Phys. Lett. **B355**, 569 (1995); S. Fajfer, Nuov. Cim. **A110**, 397 (1997).
- [20] E787 Collaboration, Phys. Rev. Lett. **79**, 2204 (1997).
- [21] A.J. Buras and R. Fleischer, hep-ph/9704376; A.J. Buras, hep-ph/9711217; G. Buchalla and A.J. Buras, Nucl. Phys. **B400**, 225 (1993); A. Ali, C. Greub and T. Mannel, DESY-93-016; G. Buchalla and A.J. Buras, M.E. Lautenbacher, Rev. Mod. Phys. **68**, 1125 (1996).
- [22] Mohammad R. Ahmady, Phys. Rev. **D53**, 2843 (1996);
- [23] CLEO Collaboration, Phys. Rev. Lett. **80**, 1150 (1998).
- [24] CLEO Collaboration, Phys. Rev. Lett. **80**, 2289 (1998).
- [25] Y. Grossman, Z. Ligeti, E. Nardi, Nucl. Phys. **B465**, 369 (1996).
- [26] A. Ali, DESY 96-106, hep-ph/9606324, and the references therein.
- [27] F. Abe et al. The CDF Collaboration, Phys. Rev. **D57**, 3811 (1998).
- [28] K. Fujikawa and A. Yamada, Phys. Rev. **D49**, 5890 (1994).

Table Captions

Table. 1.

Experimental data and predicted values of various electroweak observables in the SM and the proposed model (with different choices of parameters), for $\alpha_s = 0.118$, $m_t = 175$ GeV and $m_H = 100$ GeV.

Table. 2.

The lower bound on x derived from various decay processes for the proposed model with the d -quark mixing scenario. Case I: $\sin^2 \beta = 0$, $\sin^2 \phi = 0.04$. Case II: $\sin^2 \beta = 0.5$, $\sin^2 \phi = 0.04$.

Table. 3.

Predictions of various decay rates and mixing in the SM and the proposed model with the d -quark mixing scenario. Case I: $\sin^2 \beta = 0$, $x = 20$, $\sin^2 \phi = 0.04$. Case II: $\sin^2 \beta = 0.5$, $x = 48$, $\sin^2 \phi = 0.04$.

Table. 4.

Constraints on the quark mixing parameters from various decay processes for the proposed model with the general mixing scenario.

Figure Captions

Fig. 1.

The lower bound on the heavy Z' mass as a function of $\sin^2 \phi$ at the 2σ level. Solid curve: including all Z -pole data and assuming no lepton mixing. Dashed curve: including all Z -pole data and assuming maximal lepton mixing ($\sin^2 \beta = 0.5$). Dotted curve: only including the hadronic measurements in the fit and assuming no lepton mixing.

Fig. 2.

The lower bound on the parameter x as a function of $\sin^2 \phi$ at the 2σ level.

Solid curve: including all Z -pole data and assuming no lepton mixing.

Dashed curve: Including all data and assuming maximal lepton mixing ($\sin^2 \beta = 0.5$).

Dotted curve: Including hadronic data only and assuming no lepton mixing.

Table 1: Experimental data and predicted values of various electroweak observables in the SM and the proposed model (with different choices of parameters), for $\alpha_s = 0.118$ with $m_t = 175$ GeV and $m_H = 100$ GeV. Case a: $\sin^2 \beta = 0$, $\sin^2 \phi = 0.04$, $x = 20$, $M'_Z = 1.9$ TeV, $\Gamma'_Z = 490$ GeV. Case b: $\sin^2 \beta = 0.5$, $\sin^2 \phi = 0.04$, $x = 48$ (equivalently, $M'_Z = 2.8$ TeV, $\Gamma'_Z = 760$ GeV) Case c: $\sin^2 \beta = 0.0$, $\sin^2 \phi = 0.2$, $x = 100$ (equivalently, $M'_Z = 2$ TeV, $\Gamma'_Z = 100$ GeV)

Observables	Experimental data	SM	The model		
Included in fit			a	b	c
<u>LEP1</u>					
$g_V(e)$	-0.0367 ± 0.0015	-0.0374	-0.0374	-0.0374	-0.0375
$g_A(e)$	-0.50123 ± 0.00044	-0.50142	-0.50140	-0.50141	-0.50132
$g_V(\mu)/g_V(e)$	1.02 ± 0.12	1.00	1.00	1.01	1.02
$g_A(\mu)/g_A(e)$	0.9993 ± 0.0017	1.0000	1.0000	1.0004	1.0000
$g_V(\tau)/g_V(e)$	0.998 ± 0.060	1.000	1.027	1.006	1.027
$g_A(\tau)/g_A(e)$	0.9996 ± 0.0018	1.0000	1.0020	1.0004	1.0020
$\Gamma_Z(\text{GeV})$	2.4948 ± 0.0025	2.4972	2.4999	2.4983	2.4992
R_e	20.757 ± 0.056	20.747	20.770	20.757	20.770
R_μ	20.783 ± 0.037	20.747	20.770	20.738	20.770
R_τ	20.823 ± 0.050	20.795	20.730	20.786	20.730
$\sigma_h^0(\text{nb})$	41.486 ± 0.053	41.474	41.422	41.452	41.422
A_e	0.1399 ± 0.0073	0.1484	0.1485	0.1484	0.1487
A_τ	0.1411 ± 0.0064	0.1484	0.1521	0.1492	0.1523
A_e^{FB}	0.0160 ± 0.0024	0.0165	0.0165	0.0165	0.0166
A_μ^{FB}	0.0163 ± 0.0014	0.0165	0.0165	0.0166	0.0166
A_τ^{FB}	0.0192 ± 0.0018	0.0165	0.0169	0.0166	0.0170
R_b	0.2170 ± 0.0009	0.2157	0.2165	0.2160	0.2165
R_c	0.1734 ± 0.0048	0.1721	0.1719	0.1720	0.1719
A_{FB}^c	0.0741 ± 0.0048	0.0744	0.0744	0.0744	0.0746
<u>SLD</u>					
A_b	0.900 ± 0.050	0.935	0.935	0.935	0.935
A_c	0.650 ± 0.058	0.668	0.668	0.668	0.668
<u>Tevatron + LEP2</u>					
$M_W(\text{GeV})$	80.430 ± 0.084	80.402	80.403	80.403	80.409
<u>Not included in fit</u>					
A_{FB}^b	0.0984 ± 0.0024	0.1040	0.1041	0.1040	0.1043
A_{LR}	0.1547 ± 0.0032	0.1484	0.1485	0.1484	0.1487

Table 2: The lower bound on x derived from various decay processes for the proposed model with the d -quark mixing scenario. Case I: $\sin^2 \beta = 0$, $\sin^2 \phi = 0.04$. Case II: $\sin^2 \beta = 0.5$, $\sin^2 \phi = 0.04$.

Process	$x >$	
–	I	II
Z -Pole data	20	20
$\text{Br}(\tau^- \rightarrow \mu^- \bar{\nu}_\mu \nu_\tau) / \text{Br}(\tau^- \rightarrow e^- \bar{\nu}_e \nu_\tau)$	0	48
$\text{Br}(\tau^- \rightarrow \mu^- \mu^+ \mu^-)$	0	37
$\text{Br}(\tau \rightarrow \mu \gamma)$	0	3
$\text{Br}(K^+ \rightarrow \pi^+ \nu \bar{\nu})$	7	7
$\text{Br}(b \rightarrow s \mu^+ \mu^-)$	0	19
$\text{Br}(b \rightarrow s \nu \bar{\nu})$	15	15
$\text{Br}(B_d \rightarrow \mu^+ \mu^-)$	0	1
$\text{Br}(B_s \rightarrow \mu^+ \mu^-)$	0	4

Table 3: Predictions of various decay rates and mixing in the SM and the proposed model with the d -quark mixing scenario. Case I: $\sin^2 \beta = 0$, $x = 20$, $\sin^2 \phi = 0.04$. Case II: $\sin^2 \beta = 0.5$, $x = 48$, $\sin^2 \phi = 0.04$.

Process	Data	SM	d-type mixing	
–	–	–	I	II
$\frac{\text{Br}(\tau^- \rightarrow \mu^- \bar{\nu}_\mu \nu_\tau)}{\text{Br}(\tau^- \rightarrow e^- \bar{\nu}_e \nu_\tau)}$	0.976 ± 0.006	0.9729	0.9729	0.9881
$\text{Br}(\tau^- \rightarrow \mu^- \mu^+ \mu^-)$	$< 1.9 \times 10^{-6}$	0	0	1.1×10^{-6}
$\text{Br}(\tau \rightarrow \mu \gamma)$	$< 4.2 \times 10^{-6}$	0	0	1.7×10^{-8}
$\text{Br}(K_L^0 \rightarrow \mu^+ \mu^-)$	$(7.2 \pm 0.5) \times 10^{-9}$	$\sim 7 \times 10^{-9}$	1.3×10^{-10}	3.4×10^{-9}
$\text{Br}(K^+ \rightarrow \pi^+ \nu \bar{\nu})$	$4.2_{-3.5}^{+9.7} \times 10^{-10}$	$(9.1 \pm 3.8) \times 10^{-11}$	2.8×10^{-10}	4.8×10^{-11}
$\Delta M_K (ns^{-1})$	5.311 ± 0.019	$2.23 \sim 7.43$	$2.6 \sim 8.9$	$2.4 \sim 8.0$
$\Delta M_{B_s} (ps^{-1})$	> 10.2	$1 \sim 15$	$5 \sim 69$	$3 \sim 37$
$\text{Br}(b \rightarrow s \mu^+ \mu^-)$	$< 5.8 \times 10^{-5}$	$\sim 7 \times 10^{-6}$	1.6×10^{-7}	9.2×10^{-6}
$\text{Br}(b \rightarrow s \nu \bar{\nu})$	$< 3.9 \times 10^{-4}$	$\sim 4.2 \times 10^{-5}$	2.3×10^{-4}	4.0×10^{-5}
$\text{Br}(b \rightarrow s \mu^\pm \tau^\mp)$?	0	0	2.0×10^{-5}
$\text{Br}(B_d \rightarrow \mu^+ \mu^-)$	$< 8.6 \times 10^{-7}$	2.1×10^{-10}	3.2×10^{-11}	8.8×10^{-10}
$\text{Br}(B_s \rightarrow \mu^+ \mu^-)$	$< 2.6 \times 10^{-6}$	4.3×10^{-9}	6.1×10^{-10}	1.7×10^{-8}
$\text{Br}(B_d \rightarrow \mu^\pm \tau^\mp)$	$< 8.3 \times 10^{-4}$	0	0	4.0×10^{-7}
$\text{Br}(B_s \rightarrow \mu^\pm \tau^\mp)$?	0	0	7.7×10^{-6}
$\text{Br}(B_d \rightarrow \tau^+ \tau^-)$?	4.3×10^{-8}	2.6×10^{-6}	1.0×10^{-7}
$\text{Br}(B_s \rightarrow \tau^+ \tau^-)$?	9.1×10^{-7}	5.0×10^{-5}	2.0×10^{-6}
$\Upsilon(1S) \rightarrow \mu^\pm \tau^\mp$?	0	0	4×10^{-10}

Table 4: Constraints on the quark mixing parameters from various decay processes for the proposed model with the general mixing scenario.

Process	$\sin^2 \beta$	$\sin^2 \phi$	Constraint
$\text{Br}(K^+ \rightarrow \pi^+ \nu \bar{\nu})$	independent	independent	$ d_{31}d_{32} /x \lesssim 1.0 \times 10^{-4}$
$\text{Br}(b \rightarrow s \nu \bar{\nu})$	independent	independent	$ d_{32}d_{33} /x \lesssim 2.9 \times 10^{-3}$
$\text{Br}(b \rightarrow s \mu^+ \mu^-)$	0.5	0.04	$ d_{32}d_{33} /x \lesssim 2.3 \times 10^{-3}$
$\text{Br}(B_d \rightarrow \mu^+ \mu^-)$	0.5	0.04	$ d_{31}d_{33} /x \lesssim 9.1 \times 10^{-3}$
$\text{Br}(B_s \rightarrow \mu^+ \mu^-)$	0.5	0.04	$ d_{32}d_{33} /x \lesssim 1.2 \times 10^{-2}$